ISSN 0006-2979, Biochemistry (Moscow), 2025, Vol. 90, No. 11, pp. 1620-1642 © The Author(s) 2025. This article is an open access publication.
Published in Russian in Biokhimiya, 2025, Vol. 90, No. 11, pp. 1727-1753.

A Unique Mechanism of Glycine-Specific Inhibition of Bacterial Translation by Bottromycin A_2

Inna A. Volynkina[1,2,a]*, Aleksandr A. Grachev[3], Alexei Livenskyi[2,4,5], Daria K. Yagoda[5], Pavel S. Kasatsky[3], Olga A. Tolicheva[3], Ekaterina S. Komarova[1,6], Alexey E. Tupikin[7], Vera A. Alferova[6,8], Anastasiia O. Karakchieva[1], Arina A. Nikandrova[2,6,9], Mikhail V. Biryukov[9], Yuliya V. Zakalyukina[10], Lubov V. Dorofeeva[11], Yuriy A. Ikhalaynen[1], Igor A. Rodin[1], Dmitrii A. Lukianov[1,2], Marsel R. Kabilov[7], Alena Paleskava[3,12], Andrey L. Konevega[3,12,13,b]*, Petr V. Sergiev[1,2,6,c]*, and Olga A. Dontsova[1,2,6,8]

[1]*Department of Chemistry, Lomonosov Moscow State University, 119234 Moscow, Russia*

[2]*Center for Molecular and Cellular Biology, Skolkovo Institute of Science and Technology, 121205 Moscow, Russia*

[3]*Molecular and Radiation Biophysics Division, Petersburg Nuclear Physics Institute named by B. P. Konstantinov of National Research Center "Kurchatov Institute", 188300 Gatchina, Leningrad Region, Russia*

[4]*Institute of Gene Biology, Russian Academy of Sciences, 119334 Moscow, Russia*

[5]*Faculty of Bioengineering and Bioinformatics, Lomonosov Moscow State University, 119234 Moscow, Russia*

[6]*A. N. Belozersky Research Institute of Physico-Chemical Biology, Lomonosov Moscow State University, 119234 Moscow, Russia*

[7]*Institute of Chemical Biology and Fundamental Medicine, Siberian Branch of the Russian Academy of Sciences, 630090 Novosibirsk, Novosibirsk Oblast, Russia*

[8]*Shemyakin–Ovchinnikov Institute of Bioorganic Chemistry, Russian Academy of Sciences, 117997 Moscow, Russia*

[9]*Department of Biology, Lomonosov Moscow State University, 119234 Moscow, Russia*

[10]*Department of Soil Science, Lomonosov Moscow State University, 119234 Moscow, Russia*

[11]*All-Russian Collection of Microorganisms (VKM), G. K. Skryabin Institute of Biochemistry and Physiology of Microorganisms, Pushchino Scientific Center for Biological Research, Russian Academy of Sciences, 142290 Pushchino, Moscow Oblast, Russia*

[12]*Institute of Biomedical Systems and Biotechnologies, St. Petersburg Peter the Great Polytechnic University, 195251 Saint Petersburg, Russia*

[13]*Centre for Nano, Bio, Info, Cognitive, and Social Sciences and Technologies (NBICS Center), National Research Center "Kurchatov Institute", 123182 Moscow, Russia*

[a]*e-mail: vialabgroup@gmail.com* [b]*e-mail: konevega_al@pnpi.nrcki.ru* [c]*e-mail: petya@genebee.msu.su*

Received October 18, 2025
Revised November 6, 2025
Accepted November 6, 2025

Abstract—The rise of antimicrobial resistance among pathogenic bacteria poses a critical challenge to modern medicine, highlighting an urgent need for novel therapeutic agents. Bottromycin A_2 (BotA2) is a promising candidate for future drug development, demonstrating potent activity against clinically relevant pathogens, including methicillin-resistant *Staphylococcus aureus*, vancomycin-resistant *Enterococcus*, and *Mycoplasma* species, although its molecular mechanism of action has remained unclear until now. Here, we demonstrate that BotA2 inhibits bacterial translation with unique context specificity determined by the mRNA coding sequence. Using high-throughput toe-printing coupled with deep sequencing (Toe-seq analysis), we show that BotA2 induces ribosome pausing predominantly when a glycine codon enters the A-site of the ribosome,

* To whom correspondence should be addressed.

regardless of the codon identities in the P- and E-sites. Our biochemical and biophysical data indicate that BotA2 specifically arrests glycine-delivering ternary complexes on the ribosome, thereby preventing full accommodation of incoming Gly-$tRNA^{Gly}$ within the peptidyl transferase center. Altogether, our findings uncover a previously undescribed mechanism of translation inhibition, driven by the context-specific immobilization of ternary complexes on elongating ribosomes.

DOI: 10.1134/S0006297925603740

Keywords: bottromycin, antibiotics, translation, inhibition of protein synthesis, context specificity, ternary complex

INTRODUCTION

Bottromycin A_2 (BotA2) is a ribosomally synthesised and post-translationally modified peptide, first reported in 1957 [1]. It was purified from the fermentation broth of *Streptomyces bottropensis* and found to be active against Gram-positive bacteria [2] and *Mycoplasma* species [3, 4]. Later on, other structurally related compounds, named as bottromycin B_2 [2], C_2 [5], and D [6] were discovered. Together with BotA2, they constitute a unique class of macrocyclic peptide antibiotics – bottromycins – gaining a special interest nowadays as promising antimicrobial agents [7].

BotA2 demonstrates activity against a wide range of bacterial strains [5]. Of particular interest is the activity of BotA2 on methicillin-resistant *Staphylococcus aureus* and vancomycin-resistant *Enterococcus* [8, 9], as well as its moderate activity against *Mycobacterium* sp. and *Staphylococcus aureus* clinical isolates resistant to erythromycin, carbomycin, tetracycline, and penicillin [2, 5]. Moreover, BotA2 has proven its efficiency at combating mycoplasma infections *in vitro* [3, 4, 10], being even more potent than classical therapeutic agents, such as macrolides and tetracyclines, used for the treatment of mycoplasmosis [11]. In addition, BotA2 was also found to be active *in vitro* against the Gram-negative phytopathogenic bacterium *Xanthomonas oryzae* pv. *oryzae*, the causative agent of bacterial leaf blight of rice [12]. This emphasizes the possibility of BotA2 application in plant protection.

BotA2 is synthesized from the precursor peptide, BtmD, through a series of post-translational modifications required to ensure antibacterial activity and resistance to proteases [13]. However, the chemical structure of mature BotA2 still has an Achilles' heel, which is the labile methyl ester (marked in red in Fig. 1a) readily hydrolyzed under physiological conditions, e.g., in blood plasma, yielding a less active demethylated form of BotA2 [14]. Instability of BotA2 in oral and parenteral administration [4, 15] constitutes the main concern for introducing BotA2 into clinical practice. At the same time, antibacterial properties of BotA2 render it a promising scaffold in drug design and prompt researchers to develop more stable BotA2 derivatives [14-22]. For instance, bottromycin A_2 hydrazide is much more stable in the bloodstream and active *in vivo* against *Mycoplasma gallisepticum* in the infected chickens [4]. However, it demonstrated 8-16 times lower antibacterial activity *in vitro* compared to BotA2 [14]. Over time, the accumulated knowledge allowed characterizing structure-activity relationships of BotA2 and its derivatives, revealing that the ester and thiazole moieties could be altered, while the rest of the molecule is essential for antibacterial properties [21]. To date, only two synthesized BotA2 derivatives – propyl and ethyl ketones replacing the ester group – were shown to have both improved plasma stability and antibacterial activity comparable to that of the parental BotA2 [14]. These two compounds, especially the propyl ketone, might be considered as prospective candidates for future drug development.

While the biosynthesis and antibacterial activities of BotA2 are well studied, its molecular mechanism of action remains obscure. Previous works suggest that BotA2 inhibits translation by targeting the bacterial ribosome [23, 24]. However, there have been conflicting reports as to the ability of BotA2 to inhibit the puromycin reaction [25-28], and many proposals that BotA2 exerts its influence either through inhibiting EF-G-dependent translocation [26, 29] or through lowering the affinity of aminoacyl-tRNAs (aa-tRNAs) for the A-site [28, 30, 31]. In the earliest works, the authors noted that the activity of BotA2 highly depends on the presence of C and G nucleotides in the mRNA template [23, 25]. BotA2 was more efficient at inhibiting *in vitro* translation on poly(C), poly(UC), and poly(UG) mRNAs, compared to poly(A) and poly(U). Moreover, BotA2 was shown not to affect aminoacylation of some tRNAs ($tRNA^{Leu}$, $tRNA^{Phe}$, and $tRNA^{Pro}$) [23]. Non-enzymatic binding of aa-tRNAs (Pro-$tRNA^{Pro}$, Phe-$tRNA^{Phe}$) to ribosomes was also uninfluenced by BotA2 [23, 27, 32]. At the same time, BotA2 was able to interfere with the binding of some ternary complexes (aa-tRNA·EF-Tu·GTP) in a concentration-dependent manner, with the inhibition rate being 30-50% [30, 31]. Furthermore, BotA2 was demonstrated not to inhibit the puromycin-mediated release of nascent peptides in the *in vivo* system based on

Bacillus megaterium protoplasts [33]. Likewise, no substantial inhibition of the puromycin reaction was observed by using polysomes purified from *Escherichia coli* cells, even when the reactions were supplemented with elongation factor EF-G and GTP [31, 34]. Along with this observation, BotA2-induced inhibition of polypeptide synthesis was insensitive to the presence of EF-G·GTP, suggesting that BotA2 is unlikely to directly affect translocation [27, 30]. Not surprisingly, BotA2 was shown not to affect EF-G-dependent GTP hydrolysis [27]. Another important finding was that the presence of an excess of 50S over 30S ribosomal subunit decreased the inhibitory effect of BotA2 on polypeptide synthesis, while such an effect was not observed using an excess of 30S over 50S [24]. This indicates that BotA2 presumably interacts with the 50S ribosomal subunit. However, all previous studies do not allow one to draw an unambiguous conclusion about the detailed mechanism of translation inhibition by BotA2.

Herein we present insights into the molecular mechanism of action of BotA2. Using biochemical and biophysical approaches, we uncovered that BotA2 inhibits bacterial translation demonstrating unique context specificity determined by the mRNA coding sequence. BotA2 was found to induce ribosome stalling exclusively when a glycine codon is in the A-site of the ribosome, with stalling efficiency independent of the codon identities in the P- or E-sites. Delving into the details of BotA2 action, we identified that BotA2 does not target glycyl-tRNA synthetase and does not provoke mistranslation of glycine codons, rather completely abolishes peptide bond formation with the incoming glycine residue. Furthermore, we show that BotA2 does not interfere with EF-Tu-dependent delivery of Gly-tRNA^{Gly} to the ribosome, but instead traps the ternary complex, preventing Gly-tRNA^{Gly} from its full accommodation into the ribosomal A-site. Taking into account amino acid specificity of BotA2, our findings establish a novel, previously undescribed mechanism of translation inhibition based on specific immobilization of Gly-tRNA^{Gly} in the unaccommodated (likely A/T) state on the ribosome.

MATERIALS AND METHODS

For more details on experimental procedures, please refer to the Supplementary Methods in the Online Resource 1.

Cultivation of the producing strain, fractionation, and purification of BotA2 and BotCA. The producing strain *Streptomyces* sp. VKM Ac-2945^T was provided from the All-Russian Collection of Microorganisms, Pushchino, Russia. It was originally isolated from soil collected in the Belgorod Region in 1993. The strain was cultivated in 750 mL Erlenmeyer flasks containing 200-250 mL of soy-glycerol medium [2% soy flour, 1.5% glycerol, 0.2% yeast extract, 0.5% $CaCl_2$, 0.1% NaCl, 0.1% K_2HPO_4, tap water, pH 7.2] at 28°C with constant shaking (200 rpm, Innova® 44 Shaker, New Brunswick Scientific, USA) until the appearance of pronounced antibacterial activity (~10-12 days). The activity of fermentation broth and eluted fractions was assessed using the *E. coli* *lptD*^{mut} pDualrep2.1 reporter strain [35], as previously described [36]. The culture broth was further separated from biomass by centrifugation at 20,000*g* for 5 min and subjected to solid-phase extraction on LPS-500-H sorbent with 120 μm particle size (Technosorbent LLC, Russia) using water-acetonitrile mixtures as eluents. Active fractions, containing BotCA (eluted with 30-50% acetonitrile) and BotA2 (eluted with 75-100% acetonitrile) were collected and subjected to preparative RP-HPLC.

Preparative RP-HPLC was performed on a puriFlash® PF-4250 preparative chromatograph (Interchim, France) equipped with a VDSpher 100 C18-E (10 μm, 20×250 mm) column (VDS optilab, Germany). Chromatograms for BotA2- and BotCA-enriched fractions are provided in Fig. S1 in the Online Resource 1. The identity of the isolated compounds was first confirmed by analytical RP-HPLC using BotA2 and BotCA standards, and then by high-resolution mass spectroscopy (HRMS). HPLC-HRMS/MS analysis was performed using the Orbitrap Exploris 240 mass spectrometer coupled with the Vanquish UHPLC system (Thermo Fisher Scientific, USA), equipped with a reversed-phase Acclaim™ 120 C18 (2.2 μm, 2.1×150 mm) column (Dionex, USA). For BotCA, the observed ions were $[M–H]^-$ at m/z 807.4224 and $[M+H]^+$ at m/z 809.4366 (calculated for $C_{41}H_{60}N_8O_7S$: $[M–H]^-$ 807.4227, Δ 0.4 ppm; $[M+H]^+$ 809.4384, Δ 2 ppm). For BotA2, the observed ions were $[M–H]^-$ at m/z 821.4382 and $[M+H]^+$ at m/z 823.4528 (calculated for $C_{42}H_{62}N_8O_7S$: $[M–H]^-$ 821.4384, Δ 0.2 ppm; $[M+H]^+$ 823.4540, Δ 1.5 ppm). The MS^2 fragmentation patterns of both compounds are provided in Fig. S2 in the Online Resource 1 and display all the characteristic fragment ions, consistent with previous reports [37].

At the stage of preliminary experiments low-resolution mass spectra were recorded using the EXPEC L-Chrom MS triple quadrupole system (EXPEC Technology, China) equipped with an electrospray ionization source (ESI).

Agar diffusion assays. Agar diffusion assay on a panel of *E. coli* resistant mutants was carried out according to the reported method [36]. Agar diffusion assay using misreading error reporter systems was performed as described previously [38].

Determination of minimum inhibitory concentration (MIC). MIC values were determined using

the standard liquid broth microdilution assay [39] in 96-well sterile plates and a total volume of 100 μL per well. Minimum inhibitory concentration was defined as the lowest concentration of an examined compound at which the growth of the bacterial strain was completely inhibited. For each MIC measurement, at least two biological replicates were performed.

***In vitro* translation in bacterial cell-free systems.** Translation reactions (3 μL total volume) were carried out with the PURExpress® In vitro Protein Synthesis Kit (New England BioLabs, USA) according to the manufacturer's protocol and previously reported procedure [40]. Alternatively, the reactions (5 μL total volume) were carried out with *E. coli* S30 Extract System for Linear Templates (Promega, USA) according to the manufacturer's instructions and previously reported assay [41].

***In vitro* translation in a mammalian cell-free system.** The whole cell extract was prepared from the HEK293T cell line as described previously [42] with minor modifications: harvested cells were not treated with lysolecithin buffer. Translation reactions were carried out as reported previously [43, 44].

Toe-printing assay. Linear DNA templates RST1 and RST3 (Table S2 in the Online Resource 1) were generated by PCR using the following pairs of partially complementary primers – RST1-fwd + RST1-rev and RST3-fwd + RST3-rev, respectively (Table S1 in the Online Resource 1). DNA templates containing short ORFs (Table S2 in the Online Resource 1) were generated by PCR using the pRFPCER plasmid [45] as a template, the CER-R reverse primer (Table S1 in the Online Resource 1), and a set of different forward primers, listed in the Table S1 in the Online Resource 1. MG template was generated using the M-GGC forward primer and NEW-CER-R reverse primer. Radiolabeled NV1 and NV2 primers (Table S1 in the Online Resource 1) were used to generate cDNA fragments by reverse transcription. The toe-printing analysis of drug-dependent ribosome stalling was performed essentially as previously described [46] with some minor modifications indicated in the Supplementary Methods in the Online Resource 1.

RelE-printing assay. The RelE-printing analysis was performed in a similar way as described for the toe-printing assay, but with some modifications indicated below. The purified RelE protein (0.8 mg/mL stock solution) was kindly provided by Dr. Dmitry E. Andreev, A. N. Belozersky Institute of Physico-Chemical Biology, Lomonosov Moscow State University, Moscow, Russia [47]. RelE was diluted 1 : 10 in Pure System Buffer [9 mM $Mg(OAc)_2$, 5 mM KH_2PO_4, 95 mM potassium glutamate, 5 mM NH_4Cl, 0.5 mM $CaCl_2$, 1 mM spermidine, 8 mM 1,4-diaminobutane, 1 mM DTT, pH 7.3] prior to the experiment. For control reactions, nuclease-free water was diluted 1 : 10 in Pure System Buffer. Following the incubation of translation reactions at 37°C for 15 min, 0.5 μL of the RelE solution or the control solution was added to each sample and the incubation was continued at 37°C for 15 min. Next, 1 pmol of the [^{32}P]-labeled NV2 primer (Table S1 in the Online Resource 1) and 2 U of the AMV Reverse Transcriptase (Roche, Switzerland) were added, and reaction tubes were additionally incubated at 37°C for 15 min. The subsequent experimental procedure was exactly the same as described in the Supplementary Methods in the Online Resource 1 for the toe-printing assay.

Toe-seq assay. The Toe-seq analysis of BotA2 context specificity was performed according to the reported method [48]. Brief description of the experimental procedure and computational processing of Toe-seq data is provided in the Supplementary Methods in the Online Resource 1. Prepared NGS libraries were sequenced on the MGIseq-2000 (MGI Tech, China) at the Genomics Core Facility (ICBFM SB RAS, Novosibirsk, Russia). Parameters of the resulting Toe-seq datasets are given in the Table S3 in the Online Resource 1.

Metabolic labeling assay. Overnight culture of *E. coli lptD^{mut}* was diluted to an OD_{600} of 0.1 in MOPS minimal medium containing 0.4% glycerol without antibiotics and grown at 37°C for 1 h. Then, 50 μL of [^{32}P]-orthophosphoric acid (1 mCi/mL, 8500 Ci/mmol) was added to 1 mL of *E. coli* culture to achieve a final radioactivity of 50 μCi/mL, followed by incubation at 37°C for 50 min. Bottromicyn A_2, microcin C, and mupirocin were added to *E. coli* cells and incubation continued for 30 min at 37°C. Final concentrations of antibiotics were 20 μM for bottromycin A_2 and microcin C, and 60 μM for mupirocin, which exceed the corresponding MICs. Metabolically radiolabeled nucleotides were extracted with formic acid and subjected to thin-layer chromatography as previously reported [49], for subsequent detection by autoradiography.

Global analysis of tRNA aminoacylation level (GATRAL). Overnight culture of *E. coli lptD^{mut}* was diluted 1 : 50 in fresh Lysogeny Broth (LB) medium without antibiotics and grown at 37°C until an OD_{600} of 0.4 was reached. Bottromycin A_2, microcin C, or no additive (control) was added to *E. coli* cells, followed by an additional incubation at 37°C for 30 min. For both antibiotics, the final concentration was 20 μM, which exceeds the corresponding MICs. Then, tRNA fractions were isolated from 5 mL of culture using the Total RNA and Small RNA Isolation Kit (Biolabmix, Russia), according to the manufacturer's protocol. Aminoacyl-tRNAs were acetylated with acetic anhydride, hydrolyzed via RNase digestion, and analyzed by LC-QTOF-MS, according to the published procedure [50].

Sample preparation for self-assembled *in vitro* translation. *In vitro* translation system on the basis of individually purified components was assembled in the buffer $TAKM_7$ [50 mM Tris-HCl (pH 7.5), 70 mM NH_4Cl, 30 mM KCl, 7 mM $MgCl_2$] essentially as previously described [51] with some modifications indicated below. MG (AUG-GGC), MF (AUG-UUU), and MV (AUG-GUU) mRNAs were obtained by T7 transcription followed by purification on a HiTrap® Q HP anion exchange column (Cytiva, USA) [52]. DNA templates for *in vitro* transcription were amplified by PCR using the following pairs of primers – T7-fwd-1 + NV2 (for MG) and T7-fwd-2 + LP-rev (for MF and MV). DNA sequences of primers and templates are provided in Tables S1 and S2 in the Online Resource 1, respectively. Individual $tRNA^{Gly}$ was prepared as previously reported [53] with some modifications provided in the Supplementary Methods in the Online Resource 1. Fluorescently labeled $tRNA^{Gly}$(Prf16/17/20) was prepared exactly as described previously [54]. Aminoacylated fMet-$tRNA^{fMet}$, BODIPY-Met-$tRNA^{fMet}$, Phe-$tRNA^{Phe}$, and Val-$tRNA^{Val}$ were purified by RP-HPLC and stored at −80°C. Gly-$tRNA^{Gly}$(Prf16/17/20) was prepared immediately before ternary complex formation. For this, 10 μM $tRNA^{Gly}$(Prf16/17/20) was incubated with 0.2 mM Gly, 3 mM ATP, 2 mM DTT, 0.75 μM Gly-tRNA synthetase in the $TAKM_7$ buffer at 37°C for 40 min. Where indicated, ternary complexes were additionally incubated with bottromycin A_2 or kirromycin at 37°C for 5 min prior to the experiment. Final concentrations of antibiotics after mixing initiation complex with ternary complex were 100 μM and 150 μM for bottromycin A_2 and kirromycin, respectively.

***In vitro* synthesis of fluorescently labeled peptides.** *In vitro* synthesis of short fluorescently labeled peptides was performed essentially as recently described [52, 55] with some modifications indicated below. Linear DNA templates (0.3 pmol) were expressed in a cell-free bacterial transcription-translation coupled system using the PURExpress® Δ(aa, tRNA) Kit (New England BioLabs) in a total volume of 5 μL, according to the manufacturer's guidance. Final concentrations of reagents in translation mixtures were corrected for the sake of better representation as indicated below. Each reaction consisted of 0.8 μL of Solution A (minus aa, tRNA, from the kit), 1.2 μL of Solution B (from the kit), 0.53 μM *E. coli* Ribosomes (New England BioLabs), 0.16 μM BODIPY-Met-$tRNA^{fMet}$, 0.2 μL of uncharged tRNA (7 mg/mL), 0.3 mM L-serine (Sigma-Aldrich, USA), 0.3 mM L-glycine (Sigma-Aldrich), 2 U of RiboLock RNase Inhibitor (Thermo Fisher Scientific), 15 ng of a DNA template, and 50 μM bottromycin A_2. Negative control samples (indicated as "–") were supplemented with nuclease-free water instead of bottromycin A_2. In parallel, control reactions were assembled to synthesize the following fluorescently labeled peptides – BODIPY-Met, BODIPY-Met-Ser, BODIPY-Met-Ser-Gly, and BODIPY-Met-Ser-Gly-Phe. Control reactions consisted of 1 μL of Solution A (minus aa, tRNA, from the kit), 1.3 μL of Solution B (from the kit), 0.08 μM BODIPY-Met-$tRNA^{fMet}$, 0.35 μL of uncharged tRNA (7 mg/mL), 0.3 mM L-serine (Sigma-Aldrich), 0.3 mM L-glycine (Sigma-Aldrich), 0.3 mM L-phenylalanine (Sigma-Aldrich), 2 U of RiboLock RNase Inhibitor (Thermo Fisher Scientific), and 10 ng of a DNA template (M-AGT, M-AGT-GGC, or M-AGT-GGC-F, Table S2 in the Online Resource 1). The "BODIPY-Met" sample was supplemented with nuclease-free water instead of a DNA template. Before the addition of templates, all reaction tubes were pre-incubated at room temperature (RT) for 5 min and then placed back on ice. Following the addition of templates, reaction mixtures were incubated at 37°C for 30 min.

For the synthesis of short fluorescently labeled peptides using the self-assembled *in vitro* translation system, initiation complexes were programmed with either of the three mRNAs – MG (AUG-GGC), MF (AUG-UUU), and MV (AUG-GUU) – and assembled with BODIPY-Met-$tRNA^{fMet}$ in the P-site. Ternary complexes were assembled with the following tRNAs – Gly-$tRNA^{Gly}$, Phe-$tRNA^{Phe}$, and Val-$tRNA^{Val}$. Translation was initiated by adding 0.2 μM ternary complex to 0.1 μM initiation complex followed by incubation at 37°C for 2 min.

Translation reactions were terminated by the addition of 0.29 M $NaHCO_3$ to hydrolyze peptidyl-tRNA and release synthesized peptides, followed by incubation at 37°C for 20 min. Then, the samples were mixed with an equal volume of Formamide Loading Dye [98% formamide, 10 mM EDTA (pH 8.0), 0.1% bromophenol blue], incubated for 3 min at 70°C, and resolved in a 20×20 cm 12% PAAG containing 7 M urea in TBE buffer [90 mM Tris base, 90 mM boric acid, 2 mM EDTA, pH 8.3]. The gel was scanned using the Typhoon™ FLA 9500 Biomolecular Imager (GE Healthcare, USA). Laser of 473 nm (blue LD laser) was used for excitation and DBR1 filter of 530 ± 20 nm was used for emission. Images were processed and visualized using the Image Lab™ software (version 6.0.1, Bio-Rad Laboratories, USA).

Rapid kinetics measurements. To monitor the time course of aminoacyl-tRNA interaction with the A-site of the ribosome, we rapidly mixed either (i) 0.1 μM initiation ribosome complexes containing BODIPY-Met-$tRNA^{fMet}$ programmed with the MG mRNA with 1 μM Gly-$tRNA^{Gly}$•EF-Tu•GTP ternary complex at 20°C or (ii) 0.1 μM Gly-$tRNA^{Gly}$(Prf16/17/20)•EF-Tu•GTP ternary complex with 0.4 μM initiation ribosome complexes programmed with the same MG mRNA at 20°C. In both cases, samples were mixed

in equal volumes (60 μL). Fluorescence was recorded using SX-20 stopped-flow spectrometer (Applied Photophysics, UK). Proflavin fluorescence was excited at 460 nm, BODIPY FL fluorescence was excited at 470 nm. Fluorescence intensity was measured after passing a cut-off filter KV 495 nm (Schott, Germany) in both cases. Time courses were obtained by averaging 5-7 individual traces. Data were evaluated by fitting to a single-exponential function with a characteristic apparent rate constant (k_{app}), amplitude (A), and final signal amplitude (F_∞) according to equation $F = F_\infty + A \cdot \exp(k_{app} \cdot t)$, where F is the fluorescence at time t. Where necessary, two exponential terms were used. All calculations were performed using the GraphPad Prism software (version 9.3.1, Dotmatics, USA).

Monitoring of EF-Tu coelution with the ribosomes. Reaction mixture containing 1 μM initiation complexes programmed with the MG mRNA and 2 μM Gly-tRNA^{Gly}(Prf16/17/20)·EF-Tu·GTP ternary complex was incubated at 37°C for 2 min followed by separation on size exclusion chromatography column (BioSuite 450 Å HR SEC (8 μm, 7.8 × 300 mm), Waters, USA) in $TAKM_7$ buffer. 1 pmol of the central fraction of 70S peak was resolved by SDS-PAGE, and the presence of EF-Tu was assessed by western blotting using primary monoclonal anti-His_6 antibodies (His-Tag Antibody, Affinity Biosciences, China) and secondary horseradish peroxidase–conjugated antibodies (Goat anti-Mouse IgG (H+L) Secondary Antibody, HRP, Thermo Fisher Scientific). The bands were developed using the Clarity™ Western ECL Substrate (Bio-Rad Laboratories) and visualized using the chemiluminescence mode in the ChemiDoc™ MP Imaging System (Bio-Rad Laboratories).

RESULTS

Bottromycin A_2 selectively inhibits bacterial translation. Bottromycin A_2 (BotA2, Fig. 1a) has long

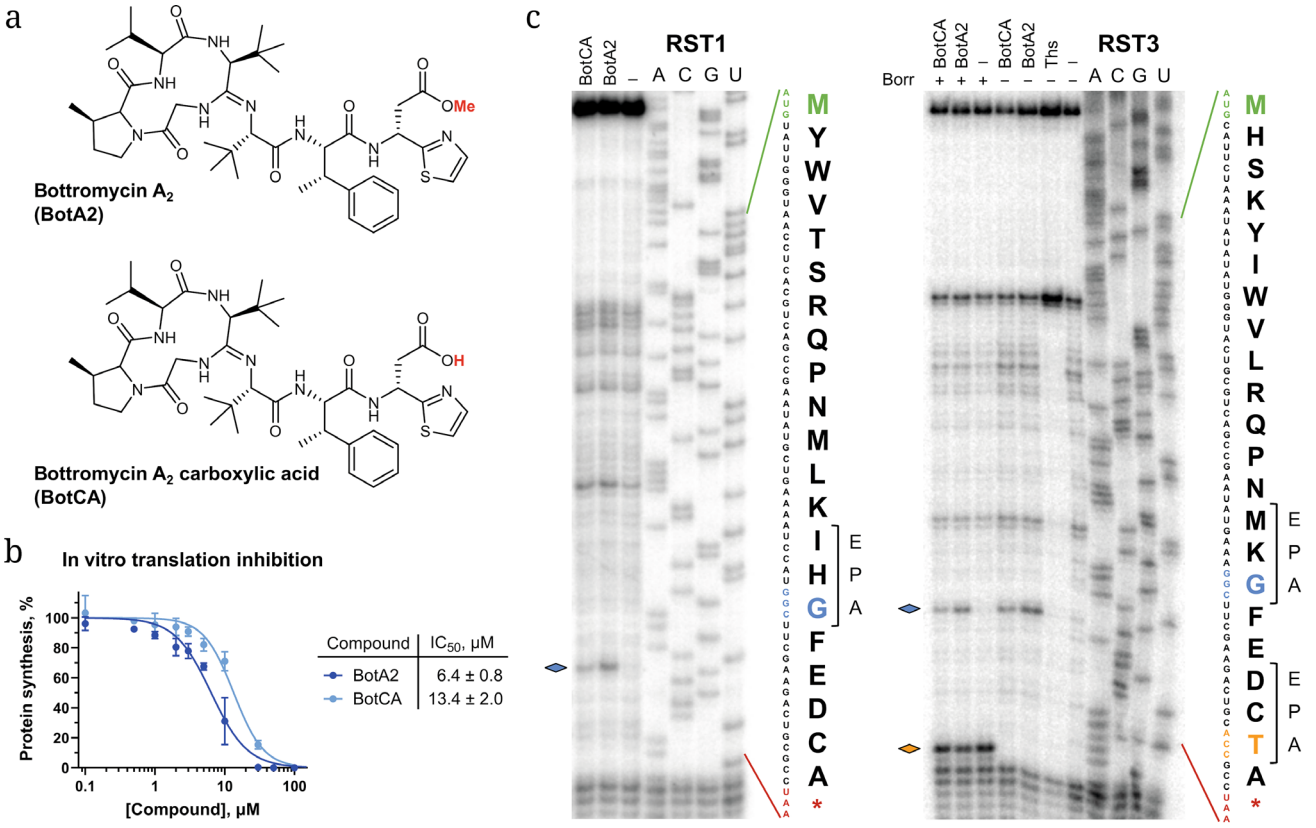

Fig. 1. Bottromycin A_2 inhibits bacterial translation in a context-specific manner. a) Chemical structures of bottromycin A_2 (BotA2) and its hydrolyzed counterpart, referred to here as bottromycin A_2 carboxylic acid (BotCA). b) BotA2 and BotCA inhibit bacterial protein synthesis *in vitro*. The efficiency of translation reaction (relative maximum Fluc accumulation rates) is plotted *vs.* antibiotic concentration. Error bars represent standard deviation, $n \geq 2$. The calculated IC_{50} values and 95% confidence intervals are shown in the table. c) Toe-printing analysis of BotA2 and BotCA on RST1 and RST3 mRNAs. Sequences of the corresponding ORFs and the encoded amino acids are shown on the right. Asterisk (*) in the translated sequence denotes a stop codon. Blue and orange diamonds mark the toe-printing bands corresponding to ribosomes stalled during translation. Codons occupying the A-site of the stalled ribosomes are highlighted in the same color. Thiostrepton (Ths) was included to map the translation start site. Borrelidin (Borr) arrests ribosomes at Thr codons. Atibiotics were added to the final concentration of 50 μM.

been known to inhibit protein synthesis in bacterial cells [23], however, the details of its action remained obscure. Since clinical application of BotA2 is limited due to the poor stability under physiological conditions, probably caused by hydrolysis of the methyl ester group [14], we were interested in comparing the action of BotA2 and its demethylated counterpart – bottromycin A_2 carboxylic acid (BotCA, Fig. 1a) – in a cell-free bacterial *in vitro* translation system. By using the commercially available PURExpress system reconstituted from purified *Escherichia coli* translation components, we observed a dose-dependent inhibition of protein synthesis by both BotA2 and BotCA, with the latter one being two-fold less efficient (IC_{50} = 6.4 ± 0.8 μM and 13.4 ± 2.0 μM, respectively, Fig. 1b). At the same time, BotCA was previously reported to exhibit 64 times less potency against Gram-positive strains compared to BotA2 [14], suggesting that the main reason for the low *in vivo* activity of BotCA may be its impaired ability to penetrate bacterial cells rather than inability to suppress translation.

By using an alternative cell-free *in vitro* system based on the *E. coli* S30 extract, we observed a strong translation inhibition by BotA2 with IC_{50} = 1.0 ± 0.1 μM (Fig. S3 in the Online Resource 1), which is comparable to other potent translation inhibitors, such as tetracenomycin X [56], chloramphenicol [57], erythromycin [58], linezolid [59], and madumycin II [60] that display IC_{50} values of 1.5 μM, 2.1 μM, 0.32 μM, 1.1 μM, and 0.3 μM, respectively. In addition, we have tested whether BotA2 and BotCA can interfere with eukaryotic mRNA translation. Both of them showed no inhibition of protein synthesis in the HEK293T whole cell lysate even at 50 μM concentrations, with BotA2 exhibiting only limited inhibitory effect at higher concentrations (500-1000 μM) (Fig. S4 in the Online Resource 1). These observations provide evidence that bottromycin A_2 specifically targets the machinery of bacterial translation.

Bottromycin A_2 does not exhibit cross-resistance to most known 50S-targeting antibiotics. Since BotA2 was shown to inhibit protein synthesis, we decided to test whether its binding site overlaps with that of other known ribosome-targeting antibiotics. By using an agar diffusion assay, we screened our homemade collection of resistant mutants for the growth inhibition induced by BotA2. Surprisingly, we have not found any *E. coli* mutant resistant to BotA2 (Fig. S5 in the Online Resource 1), which is consistent with previous works showing no cross-resistance between BotA2 and erythromycin, as well as tetracycline [5, 61]. Our data reveal that the BotA2 action is insensitive to the following nucleotide substitutions in the 23S rRNA − U1782C, G2057A, A2058G, A2059G, A2062G, U2586G, U2586C, U2609G, while they confer strong resistance to erythromycin, chloramphenicol, or tetracenomycin X (Fig. S5 in the Online Resource 1).

In addition, we checked whether the Cfr-mediated methylation of A2503 in the 23S rRNA would confer resistance to BotA2, as it has been shown for chloramphenicol, lincosamides, oxazolidinones, pleuromutilins, and streptogramins A [62]. Antibacterial activity of BotA2 was measured against the *Bacillus subtilis* 168 strain engineered to express the *cfr* gene [63], in comparison with the susceptible strain (Table S4 in the Online Resource 1). As expected, *cfr* expression resulted in an 8-fold increase in the minimum inhibitory concentration (MIC) of chloramphenicol (MIC = 100 μM). At the same time, we observed no significant differences in MIC values for BotA2 between the two *B. subtilis* strains. This result implies that BotA2 does not interact with the A2503 residue. Our reasoning is additionally supported by one of the previous works, which revealed that BotA2 does not compete with chloramphenicol for the binding site [25]. Altogether, these findings suggest that BotA2, being a potent translation inhibitor, does not share binding site with classical 50S-targeting antibiotics, but instead occupies a unique binding site.

Bottromycin A_2 inhibits translation in a context-specific manner. Since the previous investigation reported that BotA2 inhibits aminoacyl-tRNA (aa-tRNA) binding in the A-site of the ribosome [31], we decided to visualize which step of translation is inhibited by BotA2 using the toe-printing assay. Application of RST1 and RST3 mRNA templates revealed that BotA2 induces ribosome stalling during the elongation step, and specifically when a glycine (Gly) codon in the mRNA reaches the A-site of the ribosome (Fig. 1c). This observation contradicts the expectations for a conventional inhibitor of aa-tRNA accommodation, such as tetracycline, kirromycin, or lincosamides (lincomycin, clindamycin) [64]. They generate multiple toe-printing bands at the beginning of mRNA coding sequence accompanied by pronounced ribosomal arrest at the start codon [65]. Translation reactions on RST3 mRNA supplemented with borrelidine (Borr), an inhibitor of threonyl-tRNA synthetase, revealed that a fraction of ribosomes bypasses the BotA2 stalling site and becomes trapped downstream, at the Thr codon occupying the A-site (Fig. 1c). We assume that BotA2 may bind to its target reversibly, as previously proposed [25].

The obtained results prompt us to comprehensively examine the BotA2 context specificity. A recently developed high-throughput technique named Toe-seq was applied for this purpose [48]. Toe-seq uses a library of short DNA templates containing a 30-nt randomized region within its ORF. *In vitro* expression of this library using a coupled transcription-translation system in the presence of BotA2, followed

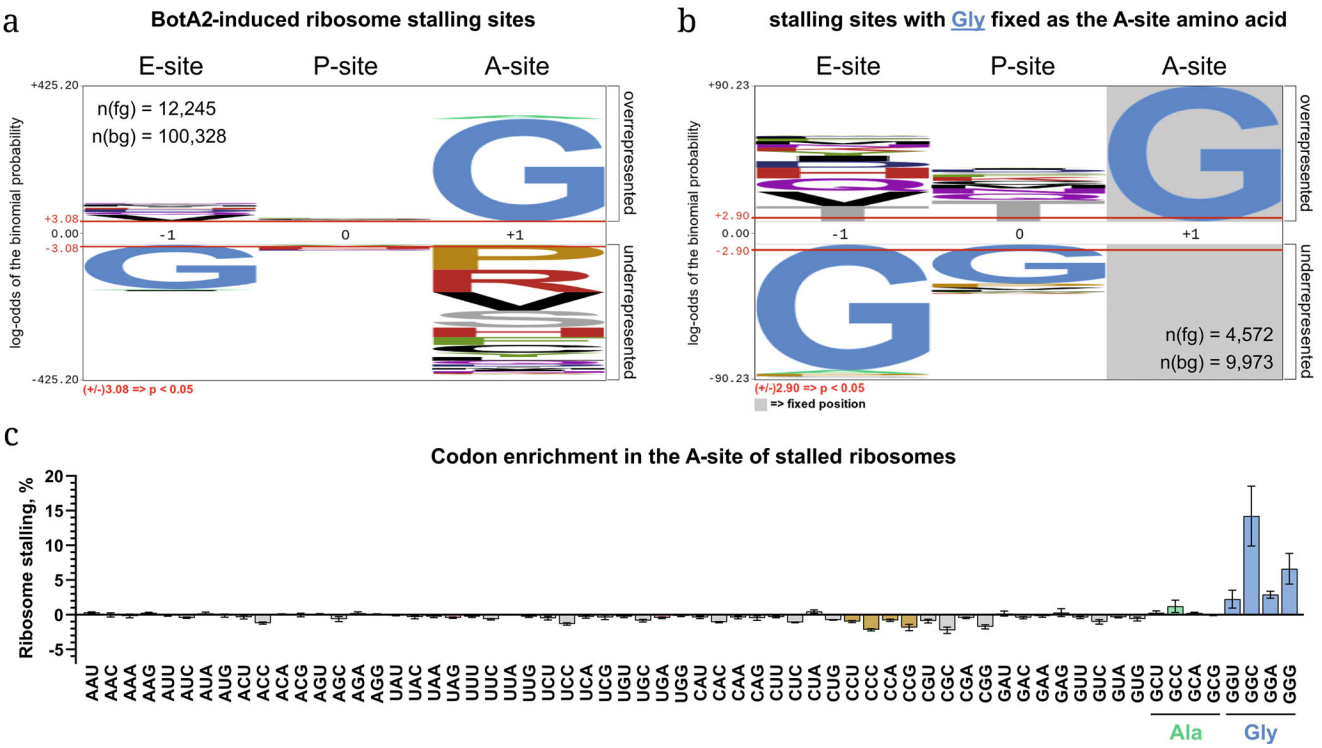

Fig. 2. Toe-seq analysis of bottromycin A_2 context specificity. a) pLogo analysis of BotA2-induced ribosome stalling sites. Amino acids corresponding to codons positioned in the E-, P-, and A-sites of arrested ribosomes are indicated. The n(fg) and n(bg) values represent the number of foreground and background sequences used to generate the image, respectively. As the foreground, we used stalling sites identified in BotA2-treated samples. As the background, we used 100,328 possible 3-aa motifs extracted from the same datasets. b) pLogo analysis of a subset of BotA2-induced ribosome stalling sites, in which glycine (Gly, G) is fixed as the A-site amino acid (position +1). a and b) Red horizontal lines on the pLogo correspond to p = 0.05. c) Enrichment of codons occupying the A-site of the ribosomes stalled in the presence of BotA2. Enrichment is shown as the mean of normalized relative occurrence of codons among 12,463 identified stalling sites in two biological replicates. Negative values conform to underrepresented codons, while positive values conform to overrepresented ones. Only codon positions 4-11 of the ORF are included in the analysis, as they correspond to the variable region of mRNA. Error bars indicate standard deviation.

by treatment with AMV reverse transcriptase resulted in multiple parallel toe-printing experiments. The generated cDNA fragments were subsequently subjected to next-generation sequencing (NGS) to identify ribosome stalling sites and map them to the mRNA library. Toe-seq analysis was performed with 50 μM BotA2 in two biological replicates along with untreated control reactions. Datasets obtained for antibiotic-treated samples were normalized to the controls and filtered according to predefined criteria (see Supplementary Methods in the Online Resource 1 for details). The resulting *MaxStallProbability* scores, representing the relative efficiency of antibiotic-induced ribosome stalling, were well correlated between both replicates (Fig. S6 in the Online Resource 1). To determine whether specific sequence signatures were associated with the sites of BotA2-mediated translation stalling, we applied pLogo analysis [66] to 12,245 sites identified in two biological replicates. Analysis of amino acid residues associated with codons occupying the E-, P-, and A-sites of arrested ribosomes revealed a strong bias toward Gly as the incoming amino acid (Fig. 2a), consistent with our earlier toe-printing experiments (Fig. 1c). Additionally, a marginal, but detectable enrichment was observed for alanine (Ala) codons positioned in the A-site. At the same time, ribosome stalling showed no clear dependence on the last or penultimate amino acid residue of the nascent polypeptide chain. Fixing Gly or Ala at the position +1 of the pLogo plot revealed some minor preferences for amino acid residues at positions −1 and 0 (Fig. 2b, Fig. S7 in the Online Resource 1). However, the significance of these preferences remains questionable and requires further validation.

We were also interested to analyze whether the efficiency of BotA2-induced ribosome stalling depends on individual codons more than on encoded amino acids. To this end, we calculated the relative occurrence of individual codons among the identified stall sites and noticed that different A-site Gly codons exhibit different stalling frequencies, with GGC being the most efficient one, followed by GGG (Fig. 2c).

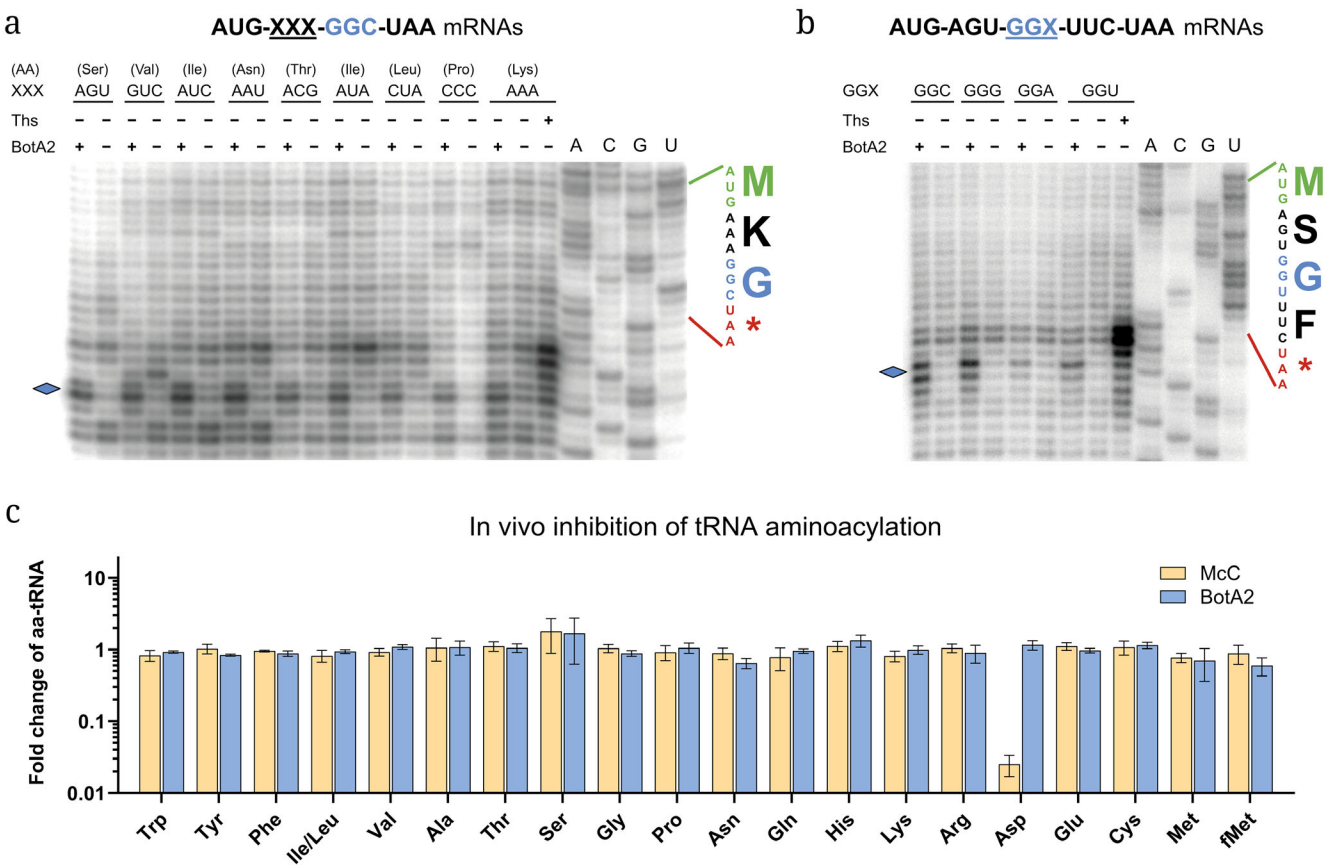

Fig. 3. Bottromycin A_2-induced ribosome stalling depends only on the identity of the A-site codon and is unrelated to inhibition of $tRNA^{Gly}$ aminoacylation. BotA2-mediated specificity of ribosomal arrest does not depend on the identity of the P-site codon (a), but depends on the identity of the A-site Gly codon (b). a and b) Toe-printing analysis of BotA2 on two sets of short mRNAs containing variable codons. Sequences of the corresponding ORFs and the encoded amino acids are shown on the right. Asterisk (*) denotes a stop codon. Blue diamonds mark the toe-printing bands corresponding to BotA2-induced ribosome stalling. Thiostrepton (Ths) was included to map the translation start site. Atibiotics were added to the final concentration of 50 μM. c) Addition of BotA2 does not change the amount of different aa-tRNAs in bacterial cells. Fold change in the level of aminoacyl-adenosines derived from aa-tRNAs that were purified from *E. coli* $lptD^{mut}$ cells treated with bottromycin A_2 (BotA2) or microcin C (McC) is shown. The values obtained for antibiotic-treated samples were normalized to the values obtained from untreated cells. Error bars represent standard deviation, n = 3.

Similarly, among the A-site Ala codons, GCC was associated with more frequent translation arrest compared to GCU, GCA, and GCG. At the same time, there was no statistically significant enrichment of codons occupying the E- and P-sites of the stalled ribosomes. These data, along with the distribution of ribosome stalling sites across the mRNA library, are provided in the Online Resource 2. Altogether, the Toe-seq analysis confirmed that BotA2 acts as a context-specific inhibitor of bacterial translation, arresting ribosomes specifically when a Gly codon occupies the A-site.

To further validate the sequence specificity of BotA2 observed in Toe-seq data, we set up a conventional toe-printing system using a set of model mRNAs. Thus, short DNA templates encoding fMet-Xxx-Gly peptides (where Xxx denotes a variable amino acid), were prepared to assess the contribution of the P-site codon to BotA2-mediated ribosome stalling. Since the GGC codon was associated with the majority of ribosome stalls, we selected it to encode Gly. Codons corresponding to the 2nd amino acid (Xxx) were randomly selected so that some of them were associated with high *MaxStallProbability* scores, while others – with medium and low scores (Fig. S8 in the Online Resource 1). Toe-printing analysis of the generated DNA templates in the presence of BotA2 revealed ribosome stalling at the 2nd position, regardless of the P-site codon identity (Fig. 3a). The absence of any reliable difference in BotA2-induced translation arrest on these templates is in agreement with our earlier Toe-seq results (Fig. 2).

Next, we checked whether the efficiency of ribosome stalling induced by BotA2 depends on the identity of Gly codons, as predicted by Toe-seq analysis (Fig. 2c). Two sets of short DNA templates were prepared to be translated into fMet-Gly-Phe and

fMet-Ser-Gly-Phe peptides, where Gly amino acid is encoded by different nucleotide triplets – GGC, GGG, GGA, or GGU. Both sets of templates showed that GGC and GGG codons were almost equally efficient, while GGU exhibited the least pronounced ribosomal arrest (Fig. 3b, Fig. S9 in the Online Resource 1). Interestingly, GGA demonstrated a strong toe-printing band, being placed at the 2nd position in ORF (Fig. S9 in the Online Resource 1), while at the 3rd position, it was much less efficient at stalling ribosomes (Fig. 3b). This observation might be related to previous results showing that GGA considerably decreases translation efficiency in *E. coli* cells, when it is placed right after the start codon, and does not alter translation being placed at the downstream positions [67, 68]. Probably, other factors unrelated to BotA2 action enhance ribosome stalling at the start codon, when Gly-tRNA^{Gly} is used as a substrate [67, 69].

Bottromycin A_2 does not inhibit glycyl-tRNA synthetase. One possible explanation of a unique sequence specificity of BotA2 action could be the inhibition of tRNA^{Gly} aminoacylation by the antibiotic. To test this hypothesis, we used two different approaches. Typical inhibitors of aminoacyl-tRNA synthetases, such as protein kinase HipA [70], microcin C [71], mupirocin [72], and serine hydroxamate [73], induce RelA-dependent synthesis of guanosine tetraphosphate (ppGpp). In cells, amino acid starvation leads to a shortage of free ternary complexes along with the accumulation of deacylated tRNAs. The RelA protein specifically recognizes an uncharged tRNA in the A-site of a stalled ribosome, acting as a sensor of amino acid deficiency [74, 75]. Upon activation, RelA converts cellular ATP and GTP/GDP to the alarmone ppGpp [76], thus inducing the stringent response aimed at the upregulation of genes involved in amino acid biosynthesis, protein hydrolysis, and transition to a so-called “hibernation” state as a means of energy conservation and survival [77-79].

By using the metabolic labeling of BotA2-susceptible *E. coli lptD^{mut}* strain, we examined whether BotA2 will induce the accumulation of ppGpp. Bacterial cells were grown in the medium supplemented with [^{32}P]-radiolabeled orthophosphoric acid, followed by treatment with BotA2. As reference agents, we used microcin C (McC) and mupirocin (Mup), inhibitors of aspartyl-tRNA [80] and isoleucyl-tRNA synthetases [81], respectively. After 30 min incubation, the labeled nucleotides were extracted with formic acid and separated via thin-layer chromatography (TLC). While McC and Mup provoked the accumulation of ppGpp in cells, BotA2 had no detectable effect (Fig. S10 in the Online Resource 1). This observation suggests that BotA2 does not increase the concentration of deacylated tRNAs and hence does not induce the stringent response.

To directly assess whether BotA2 affects the intracellular pool of aa-tRNAs, global analysis of tRNA aminoacylation level (GATRAL) [50] was performed on *E. coli lptD^{mut}* treated with BotA2. Microcin C (McC) was used as a reference agent. Total tRNA was isolated after 30 min incubation with antibiotics, followed by *N*-acetylation of aa-tRNAs to stabilize amino acid residues bound to the 3’-terminal adenosines. Then, the samples were digested with a mixture of RNase I and RNase T1 to obtain *N*-acetylated aminoacyl-adenosines (Ac-aa-Ade) that can be quantitatively analysed by LC-MS. The calculated fold change in the amount of each Ac-aa-Ade, relative to the untreated cells, reflects the abundance of the corresponding aa-tRNA in the cells (Fig. 3c). As expected, McC caused a substantial decrease in the Asp-tRNA^{Asp} level (see Asp in Fig. 3c), while BotA2 had no effect, even on Gly-tRNA^{Gly} (see Gly in Fig. 3c). This analysis confirms that BotA2 does not affect aminoacylation of tRNA^{Gly}, as well as other tRNAs.

In principle, BotA2 could theoretically target aminoacylated tRNAs directly, analogous to GNAT-family toxins that specifically modify the aminoacyl moiety [82]. However, a direct and specific interaction between this small antibiotic molecule and the acceptor stem of aa-tRNA seems mechanistically implausible. In addition, any non-*N*-acetylating modifications of amino acid residues of aa-tRNA would likely disturb the levels of acetylated glycyl-adenosines (Ac-Gly-Ade) used in the GATRAL assays, while the structural features of BotA2 (see Fig. 1a) rule out its function as an acetylating agent. Taken together, these observations strongly suggest that BotA2 neither inhibits glycyl-tRNA synthetase, nor directly modifies Gly-tRNA^{Gly}.

Bottromycin A_2 does not induce mistranslation of glycine codons. Another possible mechanism could involve BotA2 specifically preventing Gly-tRNA^{Gly} from binding to the A-site of the ribosome, increasing its availability for erroneous binding of near-cognate aa-tRNAs. If this were the case, BotA2 would be expected to provoke translational misreading of Gly codons similarly to other error-inducing antibiotics [83]. To assess the ability of BotA2 to decrease the fidelity of translation, we employed a set of reporter constructs encoding β-galactosidase variants with different substitutions at the catalytic residue Glu537. Under normal translation, reporter cells produce a defective protein uncapable of catalyzing the hydrolysis of the X-Gal substrate. However, treatment with certain antibiotics (e.g., kanamycin or streptomycin), which increase the translational error rate, allows Glu to be incorporated at the 537th position, resulting in the synthesis of active β-galactosidase, detected by an insoluble, indigo blue colored product [84]. Using an agar diffusion assay, we tested BotA2, BotCA, and reference antibiotics on these reporter strains (Fig. S11

in the Online Resource 1). As expected, we observed blue halos upon treatment with kanamycin and streptomycin, while rifampicin, an inhibitor of bacterial RNA polymerase [85], showed no coloration. Likewise, BotA2 and BotCA failed to produce blue halos, even when tested on pJC27-GGA and pJC27-GGG reporters, in which the 537th GAA codon was replaced by GGA or GGG, respectively. This observation led us to conclude that BotA2 does not provoke misreading of Gly codons.

Bottromycin A_2 does not interfere with the delivery of Gly-tRNA^{Gly} to the A-site of the ribosome. To determine a particular step of translation inhibited by BotA2, we examined whether it can specifically interfere with the delivery of Gly-tRNA^{Gly} to the A-site of the ribosome. For this purpose, we employed a modified toe-printing assay, in which translation reactions were additionally treated with the RelE toxin, known to cleave mRNA in the ribosomal A-site (Fig. 4a) [86]. Since the hydrolytic activity of RelE requires a vacant A-site, RelE-printing serves as a useful tool to monitor the occupancy of the A-site during translation [47]. Two mRNAs, whose translation is highly susceptible to BotA2-induced stalling, were selected for RelE-printing analysis of BotA2 action. As expected, we observed the RelE-prints originating from initiating and terminating ribosomes (see cleavage at the 2nd and 5th codons, Fig. 4b), since initiation complexes, pre-termination and post-termination complexes possess unoccupied A-sites [87]. Notably, the addition of thiostrepton (Ths) yielded only one RelE-print corresponding to ribosomes trapped at the start codon, consistent with the antibiotic's mode of action [88, 89]. Crucially, no RelE-prints corresponding to mRNA cleavage at Gly codons were detected. These data suggest that BotA2 allows delivery of Gly-tRNA^{Gly} to the A-site of the ribosome, thereby preventing the RelE-mediated cleavage of mRNA at Gly codons.

Bottromycin A_2 inhibits peptidyl transfer to Gly-tRNA^{Gly}. Having determined that the delivery of Gly-tRNA^{Gly} was not suppressed by BotA2, we sought to uncover which of the following steps – Gly-tRNA^{Gly} accommodation, peptide bond formation, or translocation – is affected by BotA2. Some of the previous works reported impaired translocation [26, 29], while others stated that the inhibition of a peptide bond formation may be the primary action of BotA2 [27, 28]. To discriminate between these two hypotheses, we decided to monitor peptide formation in the presence of BotA2 by employing a recently developed method based on *in vitro* synthesis of fluorescently labeled peptides [52, 55].

Short mRNAs from the previous experiments were used to synthesise BODIPY-labeled peptides in the presence of BotA2 (Fig. 4c). To reduce the effect of multiple-round translation, we decided to "freeze" translating ribosomes at the Gly codon by excluding Phe – the last amino acid in the tetrapeptide – from the reaction. To our surprise, the full-length BODIPY-Met-Ser-Gly-Phe tetrapeptide was synthesized anyway, probably due to the traces of Phe in the PURExpress Δ (aa, tRNA) Kit. Some amino acids or aminoacyl-adenylates (aa-AMP) may co-purify with aminoacyl-tRNA synthetases [90] during the kit preparation, thereby compromising our experiments with short mRNA templates. Nevertheless, after all the contaminating Phe had been depleted, we were able to observe the formation of truncated peptides originating from arrested ribosomes. In case BotA2 had inhibited translocation, we would have expected to see similar BODIPY-Met-Ser-Gly tripeptide yields regardless of the BotA2 addition. Instead, we observed the inhibition of BODIPY-Met-Ser-Gly synthesis in all reactions supplemented with BotA2 (Fig. 4c). In agreement with our earlier results (Fig. 3b), GGG and GGC codons were associated with the highest inhibitory effect, while GGU was the least efficient. The accumulation of the BODIPY-Met-Ser dipeptide along with the inhibition of BODIPY-Met-Ser-Gly synthesis indicates that BotA2 primarily inhibits peptide bond formation rather than translocation.

However, due to the traces of Phe in the PURExpress *in vitro* translation system, the real inhibition rate of peptide transfer to Gly-tRNA^{Gly} was difficult to assess. We decided to validate our observations using a reconstituted *in vitro* translation system consisting of individual purified components [52]. The reaction mixtures were assembled by combining initiating 70S ribosomes attached to the mRNA with the AUG start codon in the P-site followed by the codon directing incorporation of Gly (GGC), Phe (UUU), or Val (GUU), and the cognate ternary complex (aa-tRNA·EF-Tu·GTP), containing Gly-tRNA^{Gly}, Phe-tRNA^{Phe}, or Val-tRNA^{Val}, respectively. Consistent with the previous experiment, BotA2 prevented the formation of BODIPY-Met-Gly entirely, while it had no effect on the synthesis of BODIPY-Met-Phe and BODIPY-Met-Val (Fig. 4d). Altogether, our findings strongly suggest that BotA2 specifically impairs incorporation of glycine into a growing peptide chain.

Bottromycin A_2 prevents accommodation of Gly-tRNA^{Gly} in the peptidyl transferase center. Since peptidyl transfer to Gly-tRNA^{Gly} positioned in the A-site is impaired in the presence of BotA2, we considered whether BotA2 inhibits peptide bond formation directly or instead prevents the accommodation of Gly-tRNA^{Gly} in the peptidyl transferase center (PTC) prior to transpeptidation. To verify these possibilities, we tracked the approaching of acceptor stem of Gly-tRNA^{Gly} to the PTC. To this end, we used a stopped-flow fluorescence detection assay for monitoring the delivery of glycine in the form of the

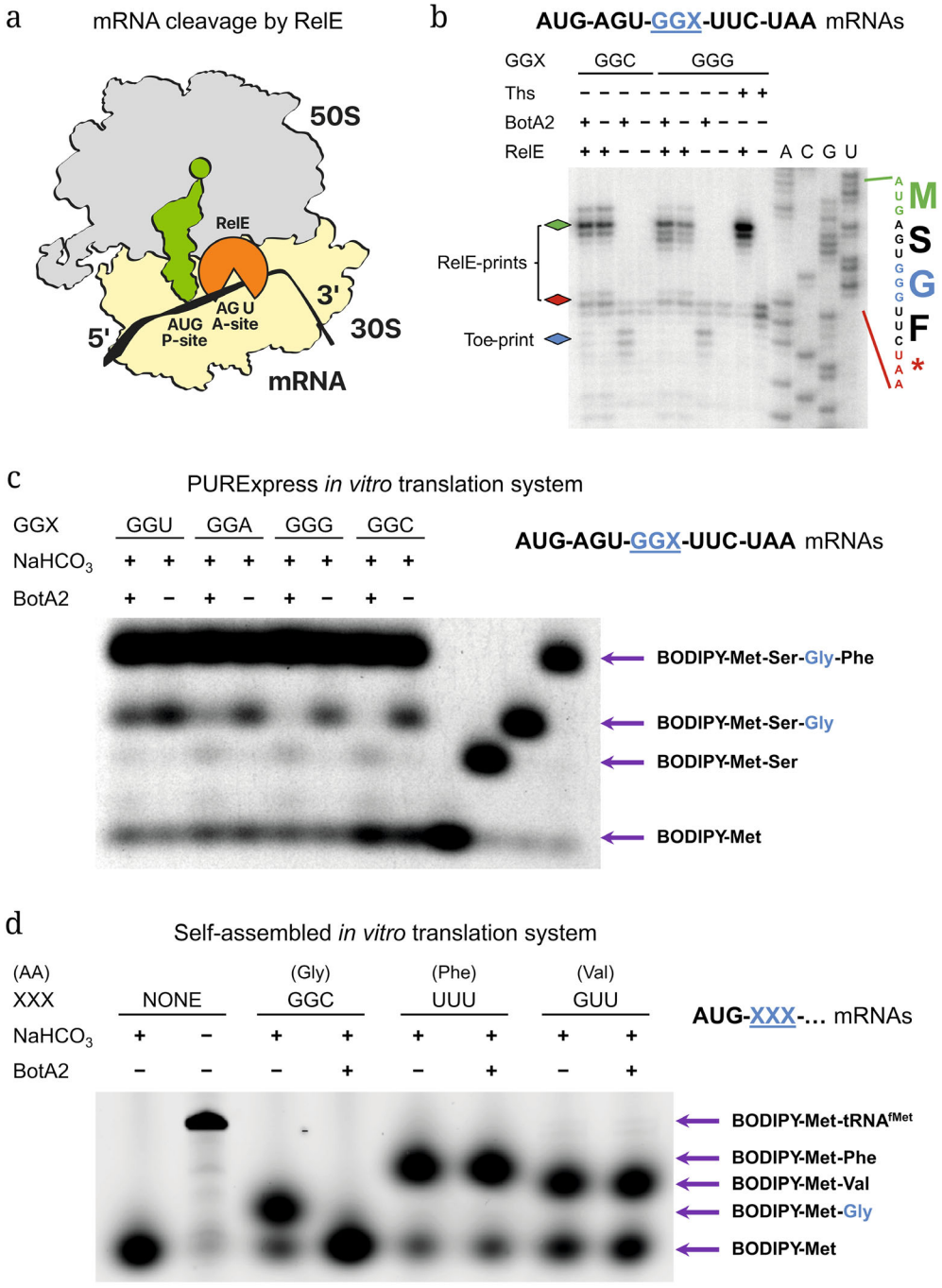

Fig. 4. Bottromycin A_2 allows delivery of Gly-tRNA^{Gly} to the A-site of the ribosome, but interferes with the peptide bond formation. a) Schematic representation of RelE-mediated cleavage of mRNA. RelE binds in the ribosomal A-site and cleaves mRNA after the 2nd or 3rd nucleotide in the A-site codon [86]. RelE does not cleave free mRNA, as well as when the A-site is occupied with aa-tRNA. b) RelE-printing analysis of BotA2-induced ribosome stalling. Toe-printing reactions supplemented with the RelE toxin indicate the position of ribosomes with the vacant A-site. Sequences of the corresponding ORFs and the encoded amino acids are shown on the right. Asterisk (*) denotes a stop codon. Blue diamond marks the toe-printing bands corresponding to BotA2-induced ribosome stalling. Green and red diamonds mark the RelE-printing bands corresponding to mRNA fragments cleaved at the 2nd and 5th codons, respectively. Thiostrepton (Ths) was included to map the translation start site. Antibiotics were added to the final concentration of 50 μM. c and d) *In vitro* synthesis of fluorescently labeled peptides using PURExpress (c) or self-assembled (d) translation system. In (c), each reaction was supplied with BODIPY-labeled fMet-tRNA^{fMet}, uncharged tRNAs, and amino acids – Ser and Gly. BotA2 was added to the final concentration of 50 μM. In (d), BODIPY-Met-Gly/Phe/Val dipeptides were formed upon addition of a pre-assembled cognate ternary complex to the 70S initiation complexes programmed with the MG (AUG-GGC), MF (AUG-UUU), or MV (AUG-GUU) mRNA and containing BODIPY-Met-tRNA^{fMet} in the P-site. Where indicated, ternary complexes were additionally incubated with 100 μM BotA2.

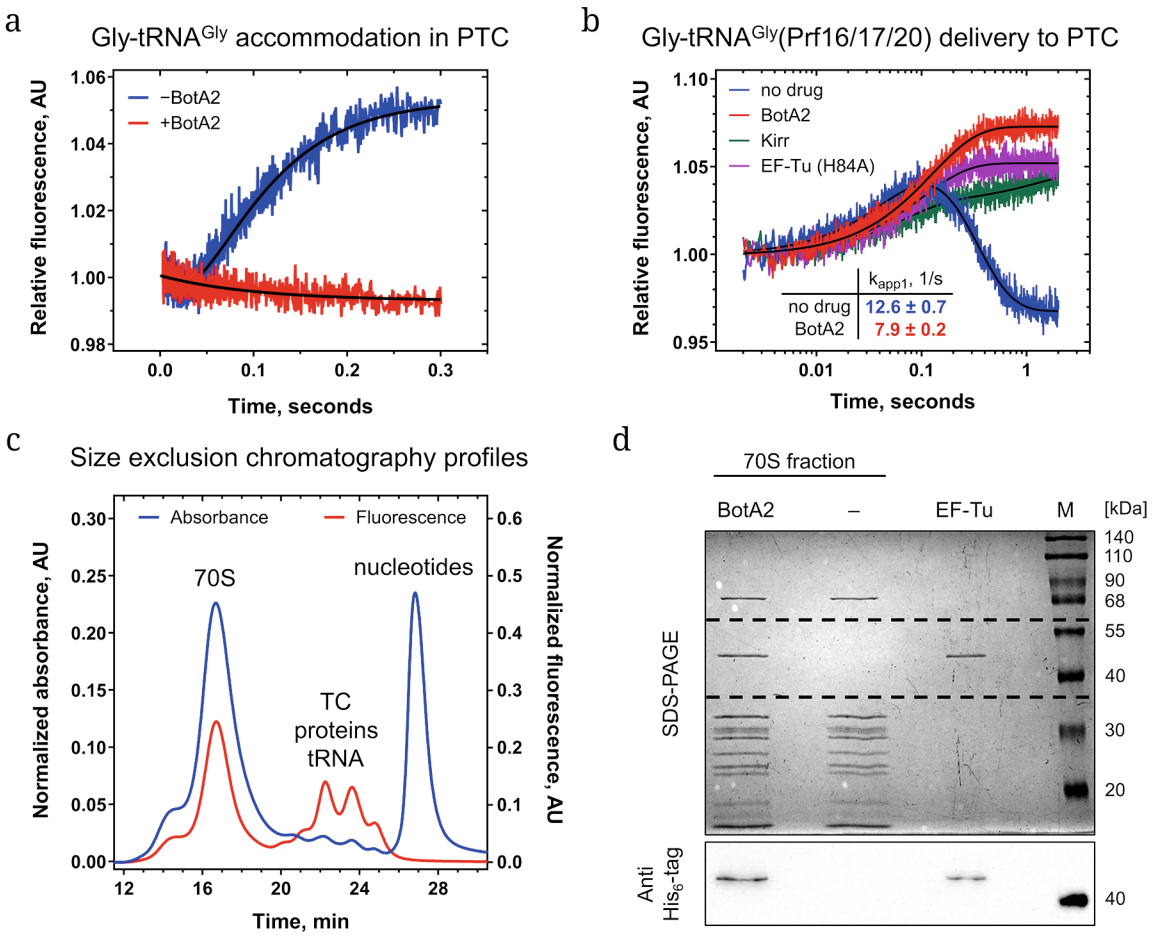

Fig. 5. Bottromycin A_2 prevents accommodation of Gly-tRNA^{Gly} in the peptidyl transferase center (PTC) by trapping ternary complex on the ribosome. a and b) Stopped-flow experiments showing that BotA2 prevents accommodation of Gly-tRNA^{Gly} in the ribosomal A-site. a) Pre-steady state kinetics of Gly-tRNA^{Gly} accommodation monitored by fluorescence change of BODIPY-Met-tRNA^{fMet} positioned in the P-site of the 70S initiation complex in the absence (blue) or presence of BotA2 (red). b) Pre-steady state kinetics of Gly-tRNA^{Gly} binding to the A-site monitored by fluorescence change of the ternary complex Gly-tRNA^{Gly}(Prf16/17/20)·EF-Tu·GTP upon interaction with the 70S initiation complex. Time courses were obtained in the absence (blue) or presence of BotA2 (red), as well as in the presence of kirromycin (Kirr, green) or modified variant of EF-Tu (His84Ala) deficient on GTP hydrolysis (purple). c and d) BotA2 impairs EF-Tu dissociation from the translating ribosome. c) Profiles of size exclusion chromatography of the 70S initiation complex after incubation with the ternary complex Gly-tRNA^{Gly}(Prf16/17/20)·EF-Tu·GTP in the presence of BotA2. Absorbance values were measured at 260 nm (blue). Fluorescence was measured using excitation at 460 nm and detection at 510 nm (red). TC, ternary complexes. d) Upper panel: SDS-PAGE of His-tagged EF-Tu (lane EF-Tu) and 70S peak fractions corresponding to ribosomal complexes assembled in the absence (lane −) or presence of BotA2 (lane BotA2). Lower panel: Immunoblotting of the area between the dashed lines with anti-His_6 antibodies. Where indicated, BotA2 was added to the final concentration of 100 μM.

ternary complex Gly-tRNA^{Gly}·EF-Tu·GTP in the vicinity of BODIPY-labeled methionine residue of initiator tRNA positioned in the P-site of the ribosome (Fig. 5a). Interestingly, for BotA2-treated complexes we did not observe the conventional increase in fluorescent signal, characteristic for the A-site accommodation of aa-tRNA acceptor end [51]. This observation allowed us to suppose that BotA2 does not inhibit peptidyl transferase reaction *per se*, but instead impairs the preceding step of amino acid delivery to the PTC.

To monitor the delivery of glycine residue in real time, we continued using the stopped-flow technique and prepared a modified tRNA^{Gly}, labeled with the fluorescent dye at the elbow region – tRNA^{Gly}(Prf16/17/20). The interaction of proflavin-labeled tRNA with the ribosomal A-site is well characterized and can be divided into several substeps [91]. An increase in a typical biphasic fluorescence kinetic curve cumulatively reflects the initial binding of the ternary complex to the ribosome, followed by codon recognition, which induces GTPase activation and results in GTP hydrolysis by EF-Tu. The subsequent decrease in fluorescence signal is related to the release of aa-tRNA from the GDP-bound form of EF-Tu and accommodation of the aa-tRNA in the ribosomal PTC (Fig. 5b). The exponential fitting of the fluorescence

kinetic curves provided apparent rate constants of the reactions preceding GTP hydrolysis and aa-tRNA accommodation. Remarkably, BotA2 slightly reduced the rate of ternary complex binding (k_{app1} (no drug) = 12.6 ± 0.7 s^{-1} *vs.* k_{app1}(BotA2) = 7.9 ± 0.2 s^{-1}), and completely abolished the following step – accommodation of Gly-$tRNA^{Gly}$.

Bottromycin A_2 arrests glycine-delivering ternary complexes on the ribosome. Taken together, our findings imply two major possibilities. The first one is that BotA2 hinders productive tRNA accommodation by forming a steric obstacle or changing the conformation of the ribosome that closes the accommodation corridor for tRNA after successful decoding and dissociation of EF-Tu. However, it is hard to imagine that the effect can be pronounced in the case of the smallest amino acid, glycine, whereas bulky amino acids, such as phenylalanine or valine, effectively pass through and participate in the peptidyl transferase reaction. The second scenario involves retention of the aa-tRNA in a bent conformation (A/T state) with anticodon bound to mRNA and the acceptor stem interacting with EF-Tu, leading to the arrest of the ternary complex on the ribosome. To discriminate between these two possibilities, we performed size exclusion chromatography of arrested ribosomal complexes, which allowed us to separate all the components according to their hydrodynamic radii. As expected, 70S ribosomes eluted first showing the largest peak visualized by absorbance at 260 nm (blue profile, Fig. 5c). Proflavin-labeled Gly-$tRNA^{Gly}$, detected by fluorescence, was present both in the ribosomal fraction and in the central part of the chromatogram corresponding to ternary complexes (TC), proteins, and tRNAs (red profile, Fig. 5c). Size exclusion chromatography profiles of untreated ribosomal complexes are provided in Fig. S12 in the Online Resource 1. To check whether EF-Tu was trapped on the ribosome upon addition of BotA2, we analyzed the ribosomal fraction by SDS-PAGE and immunoblotting with anti-His_6 antibodies against His-tagged EF-Tu (Fig. 5d). Clear EF-Tu band appeared only in the case of antibiotic-treated ribosomes, suggesting that BotA2 impairs EF-Tu dissociation from the translating ribosome.

DISCUSSION

In this study, we examined the molecular mechanism of the peptide antibiotic bottromycin A_2 (BotA2), a potent inhibitor of bacterial translation, whose mode of action has long remained obscure despite numerous reports. Here, we showed that BotA2 has unique context specificity determined by the mRNA coding sequence. We revealed that BotA2 stalls elongating ribosomes predominantly at sites where a Gly codon occupies the ribosomal A-site, with efficiency independent of the codon identities in the P- and E-sites. Looking for the explanations of this unique context specificity, we proved that BotA2 neither interferes with aminoacylation of $tRNAs^{Gly}$ nor provokes the misreading of Gly codons. At the same time, the peptide bond formation between the incoming Gly-$tRNA^{Gly}$ and the peptidyl group of the P-site-bound peptidyl-tRNA was completely abolished in the presence of BotA2. Furthermore, we demonstrated that BotA2 traps Gly-delivering ternary complexes on the ribosome, with the tRNA anticodon base-paired to the mRNA in the A-site and unaccommodated acceptor stem of Gly-$tRNA^{Gly}$ likely retained in complex with EF-Tu.

In addition, we showed that the binding site of BotA2 differs from those of other known ribosome-targeting antibiotics. Although previous study suggested that BotA2 binds to the 50S ribosomal subunit [24], it does not exhibit cross-resistance to erythromycin, chloramphenicol, tetracenomycin X, lincosamides, and other antibiotics targeting peptidyl transferase center (Fig. S5, Table S4 in the Online Resource 1). Selection of resistant mutants is considered to be the gold standard for identifying the binding site of an antibiotic. We repeatedly attempted to select *E. coli* mutants resistant to BotA2 using strains carrying either all seven rRNA operons or a single copy of them – an approach suitable for the selection of rRNA mutations. However, these efforts consistently yielded either a bacterial lawn or no viable clones (data not shown). While these observations highlight the therapeutic potential of BotA2, our findings suggest that BotA2 binds in the unique site, distinct from those of classical 50S-targeting translation inhibitors.

From this, one may assume that BotA2 interacts with the ternary complex, rather than with the ribosome itself. Several antibiotics are known to bind to elongation factors and trap them on the ribosome. For example, kirromycin restricts EF-Tu structural rearrangements and freezes the factor in its active GTP-bound conformation, even after the GTP hydrolysis, preventing aa-tRNA accommodation [92, 93]. A similar mechanism has been shown for other kirromycin-like antibiotics (e.g., aurodox, efrotomycin, factumycin) [94, 95], enacyloxin IIa [96], as well as for didemnin B and ternatin-4 targeting the eukaryotic homolog of EF-Tu – eEF1A [97, 98]. Importantly, these drugs arrest ternary complexes regardless of the tRNA identity, consistent with their binding sites at the interface of domain I (also known as G-domain) and domain III of EF-Tu or eEF1A [99-102]. The specificity of BotA2 for one particular amino acid could be reasoned by a novel and previously unreported mechanism emanating from interactions between the antibiotic and the acceptor stem of Gly-$tRNA^{Gly}$ positioned

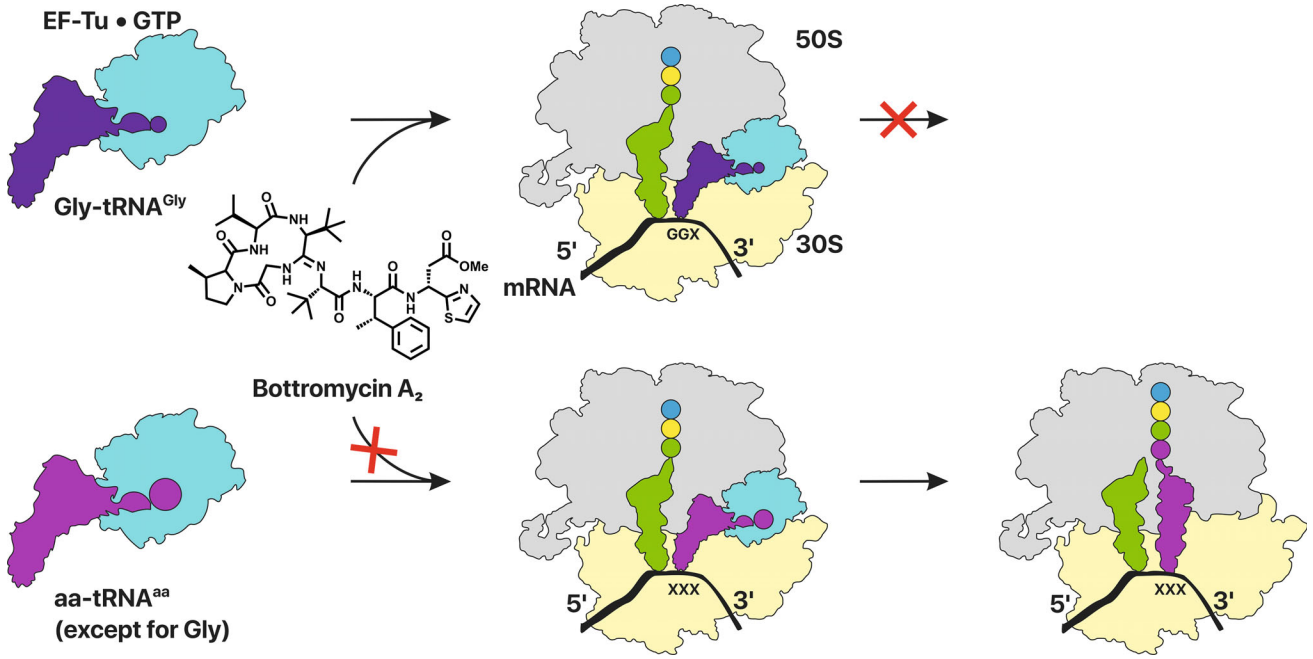

Fig. 6. The proposed mechanism of bottromycin A_2-induced ribosome stalling. Schematic diagram illustrating that bottromycin A_2 (BotA2) selectively traps glycine-delivering ternary complexes on the ribosome, preventing the accommodation of Gly-tRNA^{Gly} in the peptidyl transferase center.

in the amino acid binding pocket of EF-Tu. One could imagine that BotA2 associates only with EF-Tu, delivering the smallest amino acid, while larger incoming residues would sterically clash with the antibiotic. Being associated, BotA2 probably "glues" Gly-tRNA^{Gly} to EF-Tu, thereby impairing EF-Tu dissociation from the ribosome and preventing Gly-tRNA^{Gly} accommodation in the PTC (Fig. 6).

A comprehensive understanding of how BotA2 interacts with its target requires in-depth structural analysis complemented by genetic approaches of target validation, making the involvement of multiple research groups beneficial and essential. This study was initiated five years ago as a collaborative effort between our laboratory – including Dr. Ilya A. Osterman, who later withdrew from the project – and Prof. Rolf Müller, Dr. Joy Birkelbach (both from the Helmholtz Institute for Pharmaceutical Research, Germany), and Prof. Daniel N. Wilson (University of Hamburg, Germany). We also gratefully acknowledge our collegial interaction with Dr. Yury S. Polikanov (University of Illinois, Chicago, USA), to whom we provided our sample of BotA2 in early 2022 along with our preliminary findings. In 2025, Drs. Yury S. Polikanov and Dmitry Y. Travin (University of Illinois, Chicago, USA) reciprocated by sharing their (then) unpublished data on the structure of the BotA2-ribosome complex and BotA2 resistance mutations, which provided compelling evidence for BotA2 direct interaction with Gly-tRNA^{Gly} bound to EF-Tu [103]. Their findings complemented our own earlier results and motivated us to extend the study with the last assay detecting BotA2-induced trapping of Gly-containing ternary complexes on translating ribosomes.

Building on our initial observation of BotA2 Gly-specific activity, the combined structural, genetic, biochemical, and biophysical data from both research teams have now converged to establish a unique mechanism of translation inhibition by BotA2, involving the context-specific immobilization of ternary complexes on elongating ribosomes. This article summarizes our contributions toward clarifying the molecular details of this mechanism.

In an effort to explain why BotA2 exhibits preferences for some Gly codons, we analyzed whether this might be related to codon usage or the abundance of corresponding tRNAs (Table S5 in the Online Resource 1). In *E. coli*, codons GGU and GGC are overrepresented in highly expressed genes, while GGA and GGG are extremely underrepresented [104]. This pattern correlates well with the intracellular concentration of tRNA^{Gly} species. Three isoaccepting tRNAs^{Gly} are encoded in the *E. coli* genome [105]: codons GGC and GGU are recognized by tRNA$^{Gly}_{GCC}$ (hereafter Gly3), GGA is recognized exclusively by tRNA$^{Gly}_{UCC}$ (Gly2), while GGG is decoded by both tRNA$^{Gly}_{UCC}$ and tRNA$^{Gly}_{CCC}$ (Gly1) (Table S5 in the Online Resource 1). Consistent with codon usage, Gly3 is the most abundant tRNA^{Gly} in *E. coli* cells, followed by Gly2 and Gly1. Probably, the evolutionary depletion of GGA and GGG codons reflects their resemblance to the Shine–Dalgarno sequence, which could impede productive

translation elongation [106]. However, all these data do not correlate with the BotA2 codon preferences.

The most plausible explanation is that the strength of the codon-anticodon interaction modulates the efficiency of BotA2-induced ribosome stalling (Fig. S13 in the Online Resource 1). Apparently, perfect codon-anticodon Watson-Crick pairing stabilizes Gly-tRNA^{Gly} within the arrested complex. For example, Gly1 and Gly3 pair perfectly with GGC and GGG codons, respectively, through the formation of a total of 9 hydrogen bonds. In contrast, Gly2 forms only 8 hydrogen bonds when pairing with GGA or GGG codons. However, the 5-methylaminomethyl modification of uridine (mnm^{5}U) at the first anticodon position of Gly2 has been shown to stabilize pairing with both A and G bases [84, 107]. Therefore, the GGA and GGG recognition by Gly2 leads to the formation of only slightly less stable codon-anticodon duplexes. As such, the weakest interaction is anticipated with Gly3 pairing to GGU, which forms 8 hydrogen bonds, not stabilized by anticodon modifications (Fig. S13 in the Online Resource 1). To summarize, Gly codons can be ranked as GGC ≥ GGG > GGA > GGU, based on the strength of codon-antibodon interactions. This hierarchy correlates well with BotA2 preferences and helps to explain why GGU is the most abundant Gly codon in highly expressed genes (~60%). It is conceivable that a less stable base pairing increases the probability of Gly-tRNA^{Gly} dissociation from the ribosome as a part of a complex with EF-Tu and BotA2. Inhibition of aa-tRNA accommodation and peptide bond formation likely compels ternary complexes delivering less "sticky" Gly-tRNAs^{Gly} to undergo repeated rounds of association/dissociation, thereby increasing the ribosome's chances to bypass the stalling motif. A similar mechanism has recently been shown for chloramphenicol's action [108]. Thus, the proposed model connects the affinity of codon-anticodon base-pairing with the efficiency of BotA2-induced ribosome stalling.

Interestingly, the *btmD* gene, which encodes the bottromycin precursor peptide, begins with the evolutionary conserved ATG-GGA-CCC-... codons, translated into the fMet-Gly-Pro-... amino acid sequence [109]. Since BotA2 specifically stalls ribosomes at Gly codons, we assume that it might limit its own biosynthesis via a negative feedback loop. As previously predicted, the bottromycin (*btm*) gene cluster contains only one self-resistance gene, *btmA*, which encodes a major facilitator superfamily (MFS) transporter, probably responsible for BotA2 secretion. It is quite likely that when the concentration of BotA2 in the fermentation broth reaches a certain level, the intracellular concentration of the antibiotic also starts to increase until equilibrium. High levels of BotA2 inside the producing cells may specifically lead to downregulation of *btmD* translation, thereby inhibiting further BotA2 production to ensure cellular survival. In addition, the BtmH epimerase has been shown to bind excess BotA2 [110], presumably providing additional protection against self-poisoning [13]. On one hand, BtmH can sequester excess BotA2 with high affinity, thus lowering its free intracellular concentration. On the other hand, bound BotA2 directly inhibits BtmH, preventing further maturation of new BotA2 molecules [110]. Together, these mechanisms might control BotA2 yield upon fermentation to avoid self-harm.

As previously reported, BotA2 is not stable under physiological conditions and degrades in plasma more rapidly than it reaches the focus of inflammation [15]. At the same time, a series of BotA2 derivatives have been synthesized, some of which demonstrate both increased stability and promising antibacterial activity [14]. We hope that our work will facilitate new efforts to develop improved BotA2 derivatives, and new BotA2-based medications will soon be available for patients suffering from multidrug resistant pathogens.

Supplementary information

The online version contains supplementary materials available at https://doi.org/10.1134/S0006297925603740.

Acknowledgments

We express our sincere gratitude to Prof. Rolf Müller and Dr. Joy Birkelbach at the Helmholtz Institute for Pharmaceutical Research Saarland (HIPS) and Helmholtz Centre for Infection Research (HZI) (Saarbrücken, Germany) for providing standards for bottromycin A_2 and bottromycin A_2 carboxylic acid. We thank Prof. Daniel N. Wilson (Institute for Biochemistry and Molecular Biology, University of Hamburg, Hamburg, Germany) for cooperation in early stages of the project development and valuable discussions. We are especially grateful to Dr. Ilya A. Osterman, who originally conceived this project, for supporting early aspects of this work. We also acknowledge the work of Yury S. Polikanov (University of Illinois, Chicago, IL, USA) and his colleagues, who have shared their data ahead of publication. We also thank Andrey G. Tereshchenkov and Dr. Natalia V. Sumbatyan at the Lomonosov Moscow State University (Moscow, Russia) for helpful suggestions and attempts to reveal the binding site of bottromycin A_2. We thank Elizaveta A. Razumova for assistance with *E. coli ΔtolC* pJC27 reporter cells. We thank Dr. Dmitry E. Andreev at the A. N. Belozersky Institute of Physico-Chemical Biology (Lomonosov Moscow State University, Moscow, Russia) for providing the purified RelE protein and discussing results. We thank Tinashe P. Maviza for providing *E. coli* SQ171 strains transformed with different pLK35 and pAM552 plasmids. We thank the staff at the Skoltech Advanced Mass Spectrometry Core Facility (Moscow, Russia) for performing LC-QTOF-MS

analysis, especially Maria Zavialova and Dmitriy Maslov. Preparation of uncharged total tRNA, metabolic labeling, and analysis of aminoacylation levels of tRNAs were performed by Alexei Livenskyi, whose work was supported by the grant of Russian Science Foundation [24-14-00181]. HPLC-HRMS/MS analysis was supported by Lomonosov Moscow State University Program of Development.

Contributions

I.A.V.: validation, formal analysis, data curation, software, investigation (*in vitro* translation assays, toe-printing, RelE-printing, misreading reporter assay, synthesis of BODIPY-peptides with PURExpress system), writing – original draft, visualization, project administration. A.A.G.: formal analysis, investigation (synthesis of BODIPY-peptides with self-assembled *in vitro* translation system, rapid kinetics measurements, monitoring of EF-Tu coelution with the ribosomes). A.L.: methodology, validation, formal analysis, data curation, investigation (metabolic labeling assay, GATRAL), writing – original draft, visualization. D.K.Y.: investigation (*in vitro* translation assays, toe-printing, RelE-printing, growth inhibition of resistant mutants, synthesis of BODIPY-peptides with PURExpress system, solid-phase extraction). P.S.K.: investigation ($tRNA^{Gly}$ purification, self-assembled *in vitro* translation system). O.A.T.: investigation (synthesis of BODIPY-peptides with self-assembled *in vitro* translation system). E.S.K.: methodology, investigation (*in vitro* translation assays, Toe-seq), funding acquisition. A.E.T.: investigation (NGS). V.A.A.: methodology, validation, data curation, resources, investigation (RP-HPLC purification of BotA2 and BotCA), writing – original draft, visualization. A.O.K.: investigation (toe-printing, MIC measurement, solid-phase extraction). A.A.N.: data curation, investigation (solid-phase extraction, analytical RP-HPLC). M.V.B., Y.V.Z., and L.V.D.: methodology, investigation (cultivation of the producing strain), writing – review & editing. Y.A.I. and I.A.R.: validation, investigation (HPLC-HRMS/MS). D.A.L.: methodology, resources, writing – review & editing, project administration. M.R.K.: formal analysis, resources, data curation, software. A.P.: methodology, validation, formal analysis, data curation, writing – original draft, visualization, funding acquisition. A.L.K.: conceptualization, resources, writing – review & editing, supervision, project administration. P.V.S.: conceptualization, formal analysis, resources, writing – review & editing, supervision, project administration. O.A.D.: resources, supervision, funding acquisition. All authors read and approved the final manuscript.

Funding

This work was supported by Russian Science Foundation (RSF), grant number 21-64-00006-P to O.A.D (bacterial *in vitro* translation, toe-printing, RelE-printing, Toe-seq, experiments with bacterial cells), grant number 25-14-00253 to A.P. (experiments on self-assembled translation system, pre-steady state kinetics, and EF-Tu trapping), and grant number 24-74-00057 to E.S.K. (eukaryotic *in vitro* translation). The funders had no role in study design, data collection and analysis, decision to publish, or manuscript preparation.

Data availability

The Toe-seq sequencing data have been deposited to the NCBI BioProject database under accession number PRJNA1304769. Bioinformatics scripts are available at https://github.com/kabilov/Publication_scripts/tree/main/2024_Toe-seq. Other relevant data that support this study are available in the main manuscript, supplementary information, or from the corresponding authors upon reasonable request.

Ethics approval and consent to participate

This work does not contain any studies involving human and animal subjects.

Conflict of interest

The authors of this work declare that they have no conflicts of interest.

REFERENCES

1. Waisvisz, J. M., van der Hoeven, M. G., van Peppen, J., and Zwennis, W. C. M. (1957) Bottromycin. I. A New sulfur-containing antibiotic, *J. Am. Chem. Soc.*, **79**, 4520-4521, https://doi.org/10.1021/ja01573a072.
2. Nakamura, S., Chikaike, T., Karasawa, K., Tanaka, N., Yonehara, H., and Umezawa, H. (1965) Isolation and characterization of bottromycins A and B, *J. Antibiotics*, **18**, 47-52.

3. Miller, B. M., Stapley, E. O., and Woodruff, H. B. (1967) Antimycoplasmal activity of the bottromycin complex and its production by *Streptomyces canadensis*, *Antimicrob. Agents Chemother.*, 7, 407-414.
4. Tanaka, N., Nishimura, T., Nakamura, S., and Umezawa, H. (1968) Activity of bottromycin against *Mycoplasma gallisepticum*, *J. Antibiotics*, **21**, 75-76, https://doi.org/10.7164/antibiotics.21.75.
5. Nakamura, S., Yajima, T., Lin, Y., and Umezawa, H. (1967) Isolation and characterization of bottromycins A2, B2, C2, *J. Antibiotics*, **20**, 1-5.
6. Hou, Y., Tianero, M. D., Kwan, J. C., Wyche, T. P., Michel, C. R., Ellis, G. A., Vazquez-Rivera, E., Braun, D. R., Rose, W. E., Schmidt, E. W., and Bugni, T. S. (2012) Structure and biosynthesis of the antibiotic bottromycin D, *Organic Lett.*, **14**, 5050-5053, https://doi.org/10.1021/ol3022758.
7. Montalban-Lopez, M., Scott, T. A., Ramesh, S., Rahman, I. R., van Heel, A. J., Viel, J. H., Bandarian, V., Dittmann, E., Genilloud, O., Goto, Y., Grande Burgos, M. J., Hill, C., Kim, S., Koehnke, J., Latham, J. A., Link, A. J., Martinez, B., Nair, S. K., Nicolet, Y., Rebuffat, S., et al. (2021) New developments in RiPP discovery, enzymology and engineering, *Nat. Product Rep.*, **38**, 130-239, https://doi.org/10.1039/d0np00027b.
8. Sowa, S., Masumi, N., Inouye, Y., Nakamura, S., Takesue, Y., and Yokoyama, T. (1991) Susceptibility of methicillin-resistant *Staphylococcus aureus* clinical isolates to various antimicrobial agents, *Hiroshima J. Med. Sci.*, **40**, 137-144.
9. Shimamura, H., Gouda, H., Nagai, K., Hirose, T., Ichioka, M., Furuya, Y., Kobayashi, Y., Hirono, S., Sunazuka, T., and Omura, S. (2009) Structure determination and total synthesis of bottromycin A2: a potent antibiotic against MRSA and VRE, *Angew. Chem. Int. Ed.*, **48**, 914-917, https://doi.org/10.1002/anie.200804138.
10. Liao, Y. L. (1976) Studies on the new cell line TT-I: viral susceptibility and chromosomal changes related to mycoplasma contamination, *Chin. J. Microbiol.*, **9**, 37-44.
11. Ogata, M., Atobe, H., Kushida, H., and Yamamoto, K. (1971) *In vitro* sensitivity of mycoplasmas isolated from various animals and sewage to antibiotics and nitrofurans, *J. Antibiotics*, **24**, 443-451, https://doi.org/10.7164/antibiotics.24.443.
12. Park, S. B., Lee, I. A., Suh, J. W., Kim, J. G., and Lee, C. H. (2011) Screening and identification of antimicrobial compounds from *Streptomyces bottropensis* suppressing rice bacterial blight, *J. Microbiol. Biotechnol.*, **21**, 1236-1242, https://doi.org/10.4014/jmb.1106.06047.
13. Franz, L., Kazmaier, U., Truman, A. W., and Koehnke, J. (2021) Bottromycins - biosynthesis, synthesis and activity, *Nat. Product Rep.*, **38**, 1659-1683, https://doi.org/10.1039/d0np00097c.
14. Kobayashi, Y., Ichioka, M., Hirose, T., Nagai, K., Matsumoto, A., Matsui, H., Hanaki, H., Masuma, R., Takahashi, Y., Omura, S., and Sunazuka, T. (2010) Bottromycin derivatives: efficient chemical modifications of the ester moiety and evaluation of anti-MRSA and anti-VRE activities, *Bioorg. Med. Chem. Lett.*, **20**, 6116-6120, https://doi.org/10.1016/j.bmcl.2010.08.037.
15. Tanaka, N., Nishimura, T., Nakamura, S., and Umezawa, H. (1966) Biological studies on bottromycin A and its hydrazide, *J. Antibiotics*, **19**, 149-154.
16. Miller, W. J., Chaiet, L., Rasmussen, G., Christensen, B., Hannah, J., Miller, A. K., and Wolf, F. J. (1968) Bottromycin. Separation of biologically active compounds and preparation and testing of amide derivatives, *J. Med. Chem.*, **11**, 746-749, https://doi.org/10.1021/jm00310a603.
17. Miller, W. J., Wolf, F. J., and Chaiet, L. (1968) *A Methobottromycin and Process for Treating Poultry Infections.* Individual, USA, Patent.
18. Wolf, F. J., and Miller, W. J. (1972) *Amides of Methobottromycin.* Merck and Co Inc., USA, Patent.
19. Frost, B. M., Valiant, M. E., and Dulaney, E. L. (1979) Synergism between efrotomycin and bottromycin, *J. Antibiotics*, **32**, 1046-1049, https://doi.org/10.7164/antibiotics.32.1046.
20. Lerchen, H.-G., Schiffer, G., Brötz-Österhelt, H., Mayer-Bartschmid, A., Eckermann, S., Freiberg, C., Endermann, R., Schuhmacher, J., Meier, H., Svenstrup, N., Seip, S., Gehling, M., and Häbich, D. (2005) *Cyclic Iminopeptide Derivatives.* Aicuris Gmbh & Co. Kg, Germany, Patent.
21. Yamada, T., Yagita, M., Kobayashi, Y., Sennari, G., Shimamura, H., Matsui, H., Horimatsu, Y., Hanaki, H., Hirose, T., Omura, S., and Sunazuka, T. (2018) Synthesis and evaluation of antibacterial activity of bottromycins, *J. Org. Chem.*, **83**, 7135-7149, https://doi.org/10.1021/acs.joc.8b00045.
22. Bickel, E., and Kazmaier, U. (2024) Syntheses of bottromycin derivatives via Ugi-reactions and Matteson homologations, *Org. Biomol. Chem.*, **22**, 8811-8816, https://doi.org/10.1039/d4ob01373e.
23. Tanaka, N., Sashikata, K., Yamaguchi, H., and Umezawa, H. (1966) Inhibition of protein synthesis by bottromycin A2 and its hydrazide, *J. Biochem.*, **60**, 405-410, https://doi.org/10.1093/oxfordjournals.jbchem.a128451.
24. Kinoshita, T., and Tanaka, N. (1970) On the site of action of bottromycin A2, *J. Antibiotics*, **23**, 311-312, https://doi.org/10.7164/antibiotics.23.311.
25. Lin, Y. C., and Tanaka, N. (1968) Mechanism of action of bottromycin in polypeptide biosynthesis, *J. Biochem.*, **63**, 1-7, https://doi.org/10.1093/oxfordjournals.jbchem.a128735.
26. Lin, Y. C., Kinoshita, T., and Tanaka, N. (1968) Mechanism of protein synthesis inhibition by bottromycin A2: studies with puromycin, *J. Antibiotics*, **21**, 471-476, https://doi.org/10.7164/antibiotics.21.471.

27. Pestka, S., and Brot, N. (1971) Studies on the formation of transfer ribonucleic acid-ribosome complexes. XV. Effect of antibiotics on steps of bacterial protien synthesis: some new ribosomal inhibitors of translocation, *J. Biol. Chem.*, **246**, 7715-7722, https://doi.org/10.1016/s0021-9258(19)45834-1.
28. Otaka, T., and Kaji, A. (1981) Mode of action of bottromycin A2: effect on peptide bond formation, *FEBS Lett.*, **123**, 173-176, https://doi.org/10.1016/0014-5793(81)80280-3.
29. Tanaka, N., Lin, Y. C., and Okuyama, A. (1971) Studies on translocation of F-MET-tRNA and peptidyl-tRNA with antibiotics, *Biochem. Biophys. Res. Commun.*, **44**, 477-483, https://doi.org/10.1016/0006-291x(71)90626-7.
30. Otaka, T., and Kaji, A. (1976) Mode of action of bottromycin A2. Release of aminoacyl- or peptidyl-tRNA from ribosomes, *J. Biol. Chem.*, **251**, 2299-2306, https://doi.org/10.1016/S0021-9258(17)33586-X.
31. Otaka, T., and Kaji, A. (1983) Mode of action of bottromycin A2: effect of bottromycin A2 on polysomes, *FEBS Lett.*, **153**, 53-59, https://doi.org/10.1016/0014-5793(83)80118-5.
32. Pestka, S. (1970) Studies on the formation of transfer ribonucleic acid-ribosome complexes. IX. Effect of antibiotics on translocation and peptide bond formation, *Arch. Biochem. Biophys.*, **136**, 89-96, https://doi.org/10.1016/0003-9861(70)90330-9.
33. Cundliffe, E., and McQuillen, K. (1967) Bacterial protein synthesis: the effects of antibiotics, *J. Mol. Biol.*, **30**, 137-146, https://doi.org/10.1016/0022-2836(67)90249-5.
34. Pestka, S. (1972) Studies on transfer ribonucleic acid-ribosome complexes. XIX. Effect of antibiotics on peptidyl puromycin synthesis on polyribosoms from *Escherichia coli*, *J. Biol. Chem.*, **247**, 4669-4678, https://doi.org/10.1016/S0021-9258(19)45039-4.
35. Chernyshova, A. P., Marina, V. I., Tereshchenkov, A. G., Sagitova, V. E., Kryakvin, M. A., Dagaev, N. D., Yurchenko, E. G., Arzamazova, K. A., Guglya, E. B., Belozerova, O. A., Kovalchuk, S. I., Baranova, M. N., Kudzhaev, A. M., Shikov, A. E., Romanenko, M. N., Chebotar, V. K., Gancheva, M. S., Baganova, M. E., Biryukov, M. V., Panova, T. V., et al. (2025) Insights into the oxydifficidin's mechanism of action, *Preprints*, https://doi.org/10.20944/preprints202509.1868.v1.
36. Volynkina, I. A., Zakalyukina, Y. V., Alferova, V. A., Belik, A. R., Yagoda, D. K., Nikandrova, A. A., Buyuklyan, Y. A., Udalov, A. V., Golovin, E. V., Kryakvin, M. A., Lukianov, D. A., Biryukov, M. V., Sergiev, P. V., Dontsova, O. A., and Osterman, I. A. (2022) Mechanism-based approach to new antibiotic producers screening among actinomycetes in the course of the citizen science project, *Antibiotics*, **11**, 1198, https://doi.org/10.3390/antibiotics11091198.
37. Liu, J., Nothias, L. F., Dorrestein, P. C., Tahlan, K., and Bignell, D. R. D. (2021) Genomic and metabolomic analysis of the potato common scab pathogen *Streptomyces scabiei*, *ACS Omega*, **6**, 11474-11487, https://doi.org/10.1021/acsomega.1c00526.
38. Shapovalova, K. S., Zatonsky, G. V., Razumova, E. A., Ipatova, D. A., Lukianov, D. A., Sergiev, P. V., Grammatikova, N. E., Tikhomirov, A. S., and Shchekotikhin, A. E. (2024) Synthesis and antibacterial activity of new 6″-modified tobramycin derivatives, *Antibiotics*, **13**, 1191, https://doi.org/10.3390/antibiotics13121191.
39. Wiegand, I., Hilpert, K., and Hancock, R. E. (2008) Agar and broth dilution methods to determine the minimal inhibitory concentration (MIC) of antimicrobial substances, *Nat. Protocols*, **3**, 163-175, https://doi.org/10.1038/nprot.2007.521.
40. Paranjpe, M. N., Marina, V. I., Grachev, A. A., Maviza, T. P., Tolicheva, O. A., Paleskava, A., Osterman, I. A., Sergiev, P. V., Konevega, A. L., Polikanov, Y. S., and Gagnon, M. G. (2023) Insights into the molecular mechanism of translation inhibition by the ribosome-targeting antibiotic thermorubin, *Nucleic Acids Res.*, **51**, 449-462, https://doi.org/10.1093/nar/gkac1189.
41. Volynkina, I. A., Bychkova, E. N., Karakchieva, A. O., Tikhomirov, A. S., Zatonsky, G. V., Solovieva, S. E., Martynov, M. M., Grammatikova, N. E., Tereshchenkov, A. G., Paleskava, A., Konevega, A. L., Sergiev, P. V., Dontsova, O. A., Osterman, I. A., Shchekotikhin, A. E., and Tevyashova, A. N. (2024) Hybrid molecules of azithromycin with chloramphenicol and metronidazole: synthesis and study of antibacterial properties, *Pharmaceuticals (Basel)*, **17**, 187, https://doi.org/10.3390/ph17020187.
42. Terenin, I. M., Andreev, D. E., Dmitriev, S. E., and Shatsky, I. N. (2013) A novel mechanism of eukaryotic translation initiation that is neither m^7G-cap-, nor IRES-dependent, *Nucleic Acids Res.*, **41**, 1807-1816, https://doi.org/10.1093/nar/gks1282.
43. Akulich, K. A., Andreev, D. E., Terenin, I. M., Smirnova, V. V., Anisimova, A. S., Makeeva, D. S., Arkhipova, V. I., Stolboushkina, E. A., Garber, M. B., Prokofjeva, M. M., Spirin, P. V., Prassolov, V. S., Shatsky, I. N., and Dmitriev, S. E. (2016) Four translation initiation pathways employed by the leaderless mRNA in eukaryotes, *Sci. Rep.*, **6**, 37905, https://doi.org/10.1038/srep37905.
44. Prokhorova, I. V., Akulich, K. A., Makeeva, D. S., Osterman, I. A., Skvortsov, D. A., Sergiev, P. V., Dontsova, O. A., Yusupova, G., Yusupov, M. M., and Dmitriev, S. E. (2016) Amicoumacin A induces cancer cell death by targeting the eukaryotic ribosome, *Sci. Rep.*, **6**, 27720, https://doi.org/10.1038/srep27720.
45. Osterman, I. A., Prokhorova, I. V., Sysoev, V. O., Boykova, Y. V., Efremenkova, O. V., Svetlov, M. S., Kolb, V. A., Bogdanov, A. A., Sergiev, P. V., and Dontsova, O. A. (2012) Attenuation-based dual-fluorescent-protein reporter for screening translation inhibitors, *Antimicrob. Agents Chemother.*, **56**, 1774-1783, https://doi.org/10.1128/AAC.05395-11.

46. Orelle, C., Szal, T., Klepacki, D., Shaw, K. J., Vazquez-Laslop, N., and Mankin, A. S. (2013) Identifying the targets of aminoacyl-tRNA synthetase inhibitors by primer extension inhibition, *Nucleic Acids Res.*, **41**, e144, https://doi.org/10.1093/nar/gkt526.
47. Andreev, D., Hauryliuk, V., Terenin, I., Dmitriev, S., Ehrenberg, M., and Shatsky, I. (2008) The bacterial toxin RelE induces specific mRNA cleavage in the A site of the eukaryote ribosome, *RNA*, **14**, 233-239, https://doi.org/10.1261/rna.693208.
48. Kabilov, M. R., Komarova, E. S., Pichkur, E. B., Zotova, P. A., Kasatsky, P. S., Volynkina, I. A., Tupikin, A. E., Pavlova, J. A., Lukianov, D. A., Osterman, I. A., Pyshniy, D. V., Paleskava, A., Bogdanov, A. A., Dontsova, O. A., Konevega, A. L., and Sergiev, P. V. (2024) Context specificity of translation inhibitors revealed by toe-seq, *Res. Square*, https://doi.org/10.21203/rs.3.rs-3832009/v1.
49. Cashel, M. (1969) The control of ribonucleic acid synthesis in *Escherichia coli*. IV. Relevance of unusual phosphorylated compounds from amino acid-starved stringent strains, *J. Biol. Chem.*, **244**, 3133-3141, https://doi.org/10.1016/S0021-9258(18)93106-6.
50. Jain, I., Kolesnik, M., Kuznedelov, K., Minakhin, L., Morozova, N., Shiriaeva, A., Kirillov, A., Medvedeva, S., Livenskyi, A., Kazieva, L., Makarova, K. S., Koonin, E. V., Borukhov, S., Severinov, K., and Semenova, E. (2024) tRNA anticodon cleavage by target-activated CRISPR-Cas13a effector, *Sci. Adv.*, **10**, eadl0164, https://doi.org/10.1126/sciadv.adl0164.
51. Paleskava, A., Maksimova, E. M., Vinogradova, D. S., Kasatsky, P. S., Kirillov, S. V., and Konevega, A. L. (2021) Differential contribution of protein factors and 70S ribosome to elongation, *Int. J. Mol. Sci.*, **22**, 9614, https://doi.org/10.3390/ijms22179614.
52. Tolicheva, O. A., Bidzhieva, M. S., Kasatskiy, P. S., Marina, V. I., Sergiev, P. V., Konevega, A. L., and Paleskava, A. (2024) Separation of short fluorescently labeled peptides by gel electrophoresis for an *in vitro* translation study, *Nanobiotechnol. Rep.*, **19**, 423-431, https://doi.org/10.1134/S263516762460127X.
53. Takada, H., Crowe-McAuliffe, C., Polte, C., Sidorova, Z. Y., Murina, V., Atkinson, G. C., Konevega, A. L., Ignatova, Z., Wilson, D. N., and Hauryliuk, V. (2021) RqcH and RqcP catalyze processive poly-alanine synthesis in a reconstituted ribosome-associated quality control system, *Nucleic Acids Res.*, **49**, 8355-8369, https://doi.org/10.1093/nar/gkab589.
54. Milon, P., Konevega, A. L., Peske, F., Fabbretti, A., Gualerzi, C. O., and Rodnina, M. V. (2007) Transient kinetics, fluorescence, and FRET in studies of initiation of translation in bacteria, *Methods Enzymol.*, **430**, 1-30, https://doi.org/10.1016/S0076-6879(07)30001-3.
55. Marina, V. I., Bidzhieva, M., Tereshchenkov, A. G., Orekhov, D., Sagitova, V. E., Sumbatyan, N. V., Tashlitsky, V. N., Ferberg, A. S., Maviza, T. P., Kasatsky, P., Tolicheva, O., Paleskava, A., Polshakov, V. I., Osterman, I. A., Dontsova, O. A., Konevega, A. L., and Sergiev, P. V. (2024) An easy tool to monitor the elemental steps of *in vitro* translation via gel electrophoresis of fluorescently labeled small peptides, *RNA*, **30**, 298-307, https://doi.org/10.1261/rna.079766.123.
56. Osterman, I. A., Wieland, M., Maviza, T. P., Lashkevich, K. A., Lukianov, D. A., Komarova, E. S., Zakalyukina, Y. V., Buschauer, R., Shiriaev, D. I., Leyn, S. A., Zlamal, J. E., Biryukov, M. V., Skvortsov, D. A., Tashlitsky, V. N., Polshakov, V. I., Cheng, J., Polikanov, Y. S., Bogdanov, A. A., Osterman, A. L., Dmitriev, S. E., et al. (2020) Tetracenomycin X inhibits translation by binding within the ribosomal exit tunnel, *Nat. Chem. Biol.*, **16**, 1071-1077, https://doi.org/10.1038/s41589-020-0578-x.
57. Batool, Z., Pavlova, J. A., Paranjpe, M. N., Tereshchenkov, A. G., Lukianov, D. A., Osterman, I. A., Bogdanov, A. A., Sumbatyan, N. V., and Polikanov, Y. S. (2024) Berberine analog of chloramphenicol exhibits a distinct mode of action and unveils ribosome plasticity, *Structure*, **32**, 1429-1442.e1426, https://doi.org/10.1016/j.str.2024.06.013.
58. Pichkur, E. B., Paleskava, A., Tereshchenkov, A. G., Kasatsky, P., Komarova, E. S., Shiriaev, D. I., Bogdanov, A. A., Dontsova, O. A., Osterman, I. A., Sergiev, P. V., Polikanov, Y. S., Myasnikov, A. G., and Konevega, A. L. (2020) Insights into the improved macrolide inhibitory activity from the high-resolution cryo-EM structure of dirithromycin bound to the *E. coli* 70S ribosome, *RNA*, **26**, 715-723, https://doi.org/10.1261/rna.073817.119.
59. Grossman, T. H., Starosta, A. L., Fyfe, C., O'Brien, W., Rothstein, D. M., Mikolajka, A., Wilson, D. N., and Sutcliffe, J. A. (2012) Target- and resistance-based mechanistic studies with TP-434, a novel fluorocycline antibiotic, *Antimicrob. Agents Chemotherapy*, **56**, 2559-2564, https://doi.org/10.1128/AAC.06187-11.
60. Osterman, I. A., Khabibullina, N. F., Komarova, E. S., Kasatsky, P., Kartsev, V. G., Bogdanov, A. A., Dontsova, O. A., Konevega, A. L., Sergiev, P. V., and Polikanov, Y. S. (2017) Madumycin II inhibits peptide bond formation by forcing the peptidyl transferase center into an inactive state, *Nucleic Acids Res.*, **45**, 7507-7514, https://doi.org/10.1093/nar/gkx413.
61. Weisblum, B., and Demohn, V. (1969) Erythromycin-inducible resistance in *Staphylococcus aureus*: survey of antibiotic classes involved, *J. Bacteriol.*, **98**, 447-452, https://doi.org/10.1128/jb.98.2.447-452.1969.
62. Long, K. S., Poehlsgaard, J., Kehrenberg, C., Schwarz, S., and Vester, B. (2006) The Cfr rRNA methyltransferase confers resistance to phenicols, lincosamides, oxazolidinones, pleuromutilins, and streptogramin A antibiotics, *Antimicrob. Agents Chemotherapy*, **50**, 2500-2505, https://doi.org/10.1128/AAC.00131-06.

63. Pavlova, J. A., Khairullina, Z. Z., Tereshchenkov, A. G., Nazarov, P. A., Lukianov, D. A., Volynkina, I. A., Skvortsov, D. A., Makarov, G. I., Abad, E., Murayama, S. Y., Kajiwara, S., Paleskava, A., Konevega, A. L., Antonenko, Y. N., Lyakhovich, A., Osterman, I. A., Bogdanov, A. A., and Sumbatyan, N. V. (2021) Triphenilphosphonium analogs of chloramphenicol as dual-acting antimicrobial and antiproliferating agents, *Antibiotics*, **10**, 489, https://doi.org/10.3390/antibiotics10050489.
64. Wilson, D. N. (2009) The A-Z of bacterial translation inhibitors, *Crit. Rev. Biochem. Mol. Biol.*, **44**, 393-433, https://doi.org/10.3109/10409230903307311.
65. Orelle, C., Carlson, S., Kaushal, B., Almutairi, M. M., Liu, H., Ochabowicz, A., Quan, S., Pham, V. C., Squires, C. L., Murphy, B. T., and Mankin, A. S. (2013) Tools for characterizing bacterial protein synthesis inhibitors, *Antimicrob. Agents Chemother.*, **57**, 5994-6004, https://doi.org/10.1128/AAC.01673-13.
66. O'Shea, J. P., Chou, M. F., Quader, S. A., Ryan, J. K., Church, G. M., and Schwartz, D. (2013) pLogo: a probabilistic approach to visualizing sequence motifs, *Nat. Methods*, **10**, 1211-1212, https://doi.org/10.1038/nmeth.2646.
67. Gonzalez de Valdivia, E. I., and Isaksson, L. A. (2004) A codon window in mRNA downstream of the initiation codon where NGG codons give strongly reduced gene expression in *Escherichia coli*, *Nucleic Acids Res.*, **32**, 5198-5205, https://doi.org/10.1093/nar/gkh857.
68. Osterman, I. A., Chervontseva, Z. S., Evfratov, S. A., Sorokina, A. V., Rodin, V. A., Rubtsova, M. P., Komarova, E. S., Zatsepin, T. S., Kabilov, M. R., Bogdanov, A. A., Gelfand, M. S., Dontsova, O. A., and Sergiev, P. V. (2020) Translation at first sight: the influence of leading codons, *Nucleic Acids Res.*, **48**, 6931-6942, https://doi.org/10.1093/nar/gkaa430.
69. Johansson, M., Ieong, K. W., Trobro, S., Strazewski, P., Aqvist, J., Pavlov, M. Y., and Ehrenberg, M. (2011) pH-sensitivity of the ribosomal peptidyl transfer reaction dependent on the identity of the A-site aminoacyl-tRNA, *Proc. Natl. Acad. Sci. USA*, **108**, 79-84, https://doi.org/10.1073/pnas.1012612107.
70. Vang Nielsen, S., Turnbull, K. J., Roghanian, M., Baerentsen, R., Semanjski, M., Brodersen, D. E., Macek, B., and Gerdes, K. (2019) Serine-threonine kinases encoded by Split *hipA* homologs inhibit tryptophanyl-tRNA synthetase, *mBio*, **10**, e01138-19, https://doi.org/10.1128/mBio.01138-19.
71. Piskunova, J., Maisonneuve, E., Germain, E., Gerdes, K., and Severinov, K. (2017) Peptide-nucleotide antibiotic Microcin C is a potent inducer of stringent response and persistence in both sensitive and producing cells, *Mol. Microbiol.*, **104**, 463-471, https://doi.org/10.1111/mmi.13640.
72. Kudrin, P., Varik, V., Oliveira, S. R., Beljantseva, J., Del Peso Santos, T., Dzhygyr, I., Rejman, D., Cava, F., Tenson, T., and Hauryliuk, V. (2017) Subinhibitory concentrations of bacteriostatic antibiotics induce *relA*-dependent and *rela*-independent tolerance to beta-lactams, *Antimicrob. Agents Chemotherapy*, **61**, e02173-16, https://doi.org/10.1128/AAC.02173-16.
73. Ovchinnikov, S. V., Bikmetov, D., Livenskyi, A., Serebryakova, M., Wilcox, B., Mangano, K., Shiriaev, D. I., Osterman, I. A., Sergiev, P. V., Borukhov, S., Vazquez-Laslop, N., Mankin, A. S., Severinov, K., and Dubiley, S. (2020) Mechanism of translation inhibition by type II GNAT toxin AtaT2, *Nucleic Acids Res.*, **48**, 8617-8625, https://doi.org/10.1093/nar/gkaa551.
74. Haseltine, W. A., and Block, R. (1973) Synthesis of guanosine tetra- and pentaphosphate requires the presence of a codon-specific, uncharged transfer ribonucleic acid in the acceptor site of ribosomes, *Proc. Natl. Acad. Sci. USA*, **70**, 1564-1568, https://doi.org/10.1073/pnas.70.5.1564.
75. Sinha, A. K., and Winther, K. S. (2021) The RelA hydrolase domain acts as a molecular switch for (p)ppGpp synthesis, *Commun. Biol.*, **4**, 434, https://doi.org/10.1038/s42003-021-01963-z.
76. Hauryliuk, V., Atkinson, G. C., Murakami, K. S., Tenson, T., and Gerdes, K. (2015) Recent functional insights into the role of (p)ppGpp in bacterial physiology, *Nat. Rev. Microbiol.*, **13**, 298-309, https://doi.org/10.1038/nrmicro3448.
77. Dabrowska, G., Prusinska, J., and Goc, A. (2006) The stringent response – bacterial mechanism of an adaptive stress response [in Polish], *Postepy Biochem.*, **52**, 87-93.
78. Potrykus, K., and Cashel, M. (2008) (p)ppGpp: still magical? *Annu. Rev. Microbiol.*, **62**, 35-51, https://doi.org/10.1146/annurev.micro.62.081307.162903.
79. Urwin, L., Savva, O., and Corrigan, R. M. (2024) Microbial primer: what is the stringent response and how does it allow bacteria to survive stress? *Microbiology*, **170**, 001483, https://doi.org/10.1099/mic.0.001483.
80. Metlitskaya, A., Kazakov, T., Kommer, A., Pavlova, O., Praetorius-Ibba, M., Ibba, M., Krasheninnikov, I., Kolb, V., Khmel, I., and Severinov, K. (2006) Aspartyl-tRNA synthetase is the target of peptide nucleotide antibiotic Microcin C, *J. Biol. Chem.*, **281**, 18033-18042, https://doi.org/10.1074/jbc.M513174200.
81. Hughes, J., and Mellows, G. (1978) Inhibition of isoleucyl-transfer ribonucleic acid synthetase in *Escherichia coli* by pseudomonic acid, *Biochem. J.*, **176**, 305-318, https://doi.org/10.1042/bj1760305.
82. Bikmetov, D., Hall, A. M. J., Livenskyi, A., Gollan, B., Ovchinnikov, S., Gilep, K., Kim, J. Y., Larrouy-Maumus, G., Zgoda, V., Borukhov, S., Severinov, K., Helaine, S., and Dubiley, S. (2022) GNAT toxins evolve toward narrow tRNA target specificities, *Nucleic Acids Res.*, **50**, 5807-5817, https://doi.org/10.1093/nar/gkac356.

83. Giuliodori, A. M., Spurio, R., Milon, P., and Fabbretti, A. (2018) Antibiotics targeting the 30S ribosomal subunit: a lesson from nature to find and develop new drugs, *Curr. Top. Med. Chem.*, **18**, 2080-2096, https://doi.org/10.2174/1568026618666181025092546.
84. Manickam, N., Joshi, K., Bhatt, M. J., and Farabaugh, P. J. (2016) Effects of tRNA modification on translational accuracy depend on intrinsic codon-anticodon strength, *Nucleic Acids Res.*, **44**, 1871-1881, https://doi.org/10.1093/nar/gkv1506.
85. Campbell, E. A., Korzheva, N., Mustaev, A., Murakami, K., Nair, S., Goldfarb, A., and Darst, S. A. (2001) Structural mechanism for rifampicin inhibition of bacterial RNA polymerase, *Cell*, **104**, 901-912, https://doi.org/10.1016/s0092-8674(01)00286-0.
86. Pedersen, K., Zavialov, A. V., Pavlov, M. Y., Elf, J., Gerdes, K., and Ehrenberg, M. (2003) The bacterial toxin RelE displays codon-specific cleavage of mRNAs in the ribosomal A site, *Cell*, **112**, 131-140, https://doi.org/10.1016/s0092-8674(02)01248-5.
87. Rodnina, M. V. (2018) Translation in prokaryotes, *Cold Spring Harb. Perspect. Biol.*, **10**, a032664, https://doi.org/10.1101/cshperspect.a032664.
88. Walter, J. D., Hunter, M., Cobb, M., Traeger, G., and Spiegel, P. C. (2012) Thiostrepton inhibits stable 70S ribosome binding and ribosome-dependent GTPase activation of elongation factor G and elongation factor 4, *Nucleic Acids Res.*, **40**, 360-370, https://doi.org/10.1093/nar/gkr623.
89. Bailly, C. (2022) The bacterial thiopeptide thiostrepton. An update of its mode of action, pharmacological properties and applications, *Eur. J. Pharmacol.*, **914**, 174661, https://doi.org/10.1016/j.ejphar.2021.174661.
90. Cvetesic, N., and Gruic-Sovulj, I. (2017) Synthetic and editing reactions of aminoacyl-tRNA synthetases using cognate and non-cognate amino acid substrates, *Methods*, **113**, 13-26, https://doi.org/10.1016/j.ymeth.2016.09.015.
91. Pape, T., Wintermeyer, W., and Rodnina, M. V. (1998) Complete kinetic mechanism of elongation factor Tu-dependent binding of aminoacyl-tRNA to the A site of the *E. coli* ribosome, *EMBO J.*, **17**, 7490-7497, https://doi.org/10.1093/emboj/17.24.7490.
92. Scarano, G., Krab, I. M., Bocchini, V., and Parmeggiani, A. (1995) Relevance of histidine-84 in the elongation factor Tu GTPase activity and in poly(Phe) synthesis: its substitution by glutamine and alanine, *FEBS Lett.*, **365**, 214-218, https://doi.org/10.1016/0014-5793(95)00469-p.
93. Rodnina, M. V., Fricke, R., Kuhn, L., and Wintermeyer, W. (1995) Codon-dependent conformational change of elongation factor Tu preceding GTP hydrolysis on the ribosome, *EMBO J.*, **14**, 2613-2619, https://doi.org/10.1002/j.1460-2075.1995.tb07259.x.
94. Parmeggiani, A., and Swart, G. W. (1985) Mechanism of action of kirromycin-like antibiotics, *Annu. Rev. Microbiol.*, **39**, 557-577, https://doi.org/10.1146/annurev.mi.39.100185.003013.
95. Prezioso, S. M., Brown, N. E., and Goldberg, J. B. (2017) Elfamycins: inhibitors of elongation factor-Tu, *Mol. Microbiol.*, **106**, 22-34, https://doi.org/10.1111/mmi.13750.
96. Parmeggiani, A., Krab, I. M., Watanabe, T., Nielsen, R. C., Dahlberg, C., Nyborg, J., and Nissen, P. (2006) Enacyloxin IIa pinpoints a binding pocket of elongation factor Tu for development of novel antibiotics, *J. Biol. Chem.*, **281**, 2893-2900, https://doi.org/10.1074/jbc.m505951200.
97. Li, L. H., Timmins, L. G., Wallace, T. L., Krueger, W. C., Prairie, M. D., and Im, W. B. (1984) Mechanism of action of didemnin B, a depsipeptide from the sea, *Cancer Lett.*, **23**, 279-288, https://doi.org/10.1016/0304-3835(84)90095-8.
98. Carelli, J. D., Sethofer, S. G., Smith, G. A., Miller, H. R., Simard, J. L., Merrick, W. C., Jain, R. K., Ross, N. T., and Taunton, J. (2015) Ternatin and improved synthetic variants kill cancer cells by targeting the elongation factor-1A ternary complex, *Elife*, **4**, e10222, https://doi.org/10.7554/elife.10222.
99. Schmeing, T. M., Voorhees, R. M., Kelley, A. C., Gao, Y. G., Murphy, F. V. t., Weir, J. R., and Ramakrishnan, V. (2009) The crystal structure of the ribosome bound to EF-Tu and aminoacyl-tRNA, *Science*, **326**, 688-694, https://doi.org/10.1126/science.1179700.
100. Fischer, N., Neumann, P., Konevega, A. L., Bock, L. V., Ficner, R., Rodnina, M. V., and Stark, H. (2015) Structure of the *E. coli* ribosome-EF-Tu complex at <3 Å resolution by Cs-corrected cryo-EM, *Nature*, **520**, 567-570, https://doi.org/10.1038/nature14275.
101. Shao, S., Murray, J., Brown, A., Taunton, J., Ramakrishnan, V., and Hegde, R. S. (2016) Decoding mammalian ribosome-mRNA states by translational GTPase complexes, *Cell*, **167**, 1229-1240.e1215, https://doi.org/10.1016/j.cell.2016.10.046.
102. Juette, M. F., Carelli, J. D., Rundlet, E. J., Brown, A., Shao, S., Ferguson, A., Wasserman, M. R., Holm, M., Taunton, J., and Blanchard, S. C. (2022) Didemnin B and ternatin-4 differentially inhibit conformational changes in eEF1A required for aminoacyl-tRNA accommodation into mammalian ribosomes, *Elife*, **11**, e81608, https://doi.org/10.7554/elife.81608.
103. Travin, D. Y., Basu, R. S., Paranjpe, M. N., Klepacki, D., Zhurakovskaya, A. I., Vázquez-Laslop, N., Mankin, A. S., Polikanov, Y. S., and Gagnon, M. G. (2025) Sequence-specific trapping of EF-Tu/glycyl-tRNA complex on the ribosome by bottromycin, *bioRxiv*, https://doi.org/10.1101/2025.08.17.670399.
104. Zaytsev, K., Bogatyreva, N., and Fedorov, A. (2024) Link between individual codon frequencies and protein expression: going beyond codon adaptation index, *Int. J. Mol. Sci.*, **25**, 11622, https://doi.org/10.3390/ijms252111622.

105. Dong, H., Nilsson, L., and Kurland, C. G. (1996) Co-variation of tRNA abundance and codon usage in *Escherichia coli* at different growth rates, *J. Mol. Biol.*, **260**, 649-663, https://doi.org/10.1006/jmbi.1996.0428.
106. Rodnina, M. V. (2016) The ribosome in action: tuning of translational efficiency and protein folding, *Protein Sci.*, **25**, 1390-1406, https://doi.org/10.1002/pro.2950.
107. Kurata, S., Weixlbaumer, A., Ohtsuki, T., Shimazaki, T., Wada, T., Kirino, Y., Takai, K., Watanabe, K., Ramakrishnan, V., and Suzuki, T. (2008) Modified uridines with C5-methylene substituents at the first position of the tRNA anticodon stabilize U•G wobble pairing during decoding, *J. Biol. Chem.*, **283**, 18801-18811, https://doi.org/10.1074/jbc.M800233200.
108. Choi, J., Marks, J., Zhang, J., Chen, D. H., Wang, J., Vazquez-Laslop, N., Mankin, A. S., and Puglisi, J. D. (2020) Dynamics of the context-specific translation arrest by chloramphenicol and linezolid, *Nat. Chem. Biol.*, **16**, 310-317, https://doi.org/10.1038/s41589-019-0423-2.
109. Vior, N. M., Cea-Torrescassana, E., Eyles, T. H., Chandra, G., and Truman, A. W. (2020) Regulation of bottromycin biosynthesis involves an internal transcriptional start site and a cluster-situated modulator, *Front. Microbiol.*, **11**, 495, https://doi.org/10.3389/fmicb.2020.00495.
110. Sikandar, A., Franz, L., Adam, S., Santos-Aberturas, J., Horbal, L., Luzhetskyy, A., Truman, A. W., Kalinina, O. V., and Koehnke, J. (2020) The bottromycin epimerase BotH defines a group of atypical alpha/beta-hydrolase-fold enzymes, *Nat. Chem. Biol.*, **16**, 1013-1018, https://doi.org/10.1038/s41589-020-0569-y.